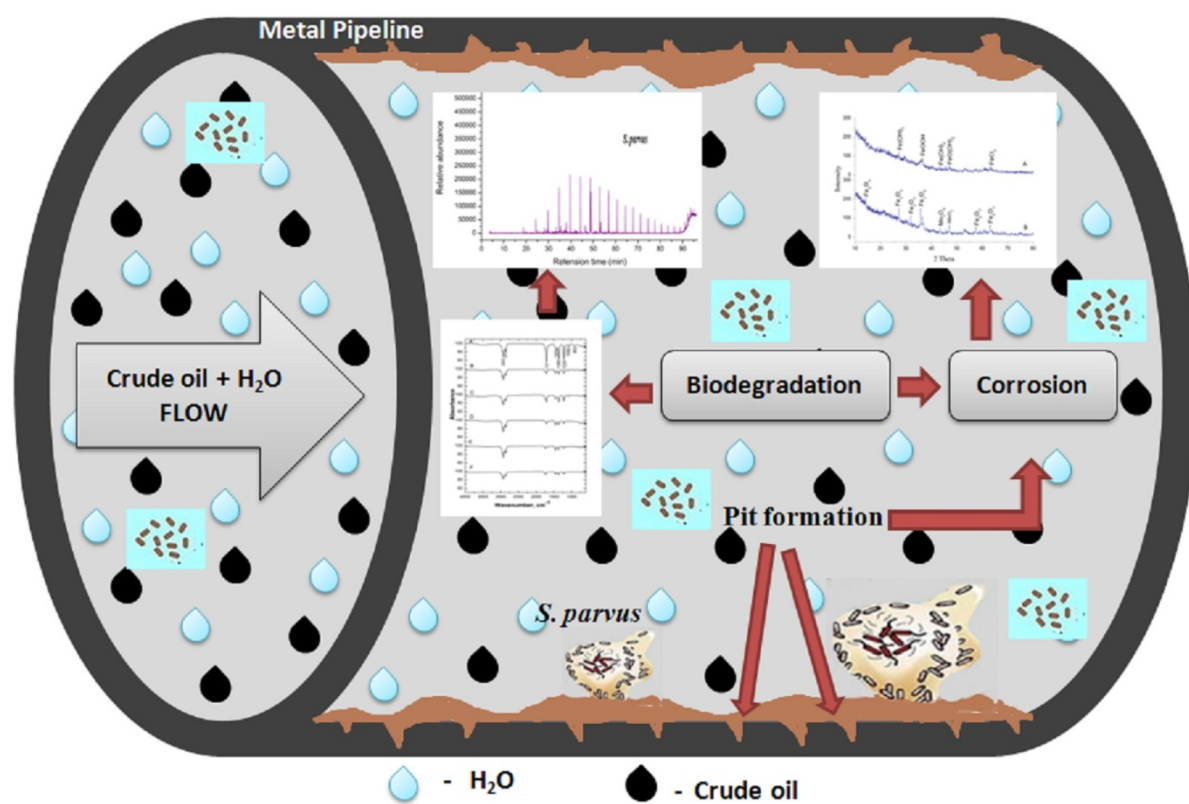


HIGHLIGHTS

- Hydrocarbon degrading bacteria were isolated from deep crude oil reservoir sediment (2000 m).
- Biosurfactant plays a key role for the utilization of crude oil.
- *Streptomyces parvus* B7 was identified as a potent crude oil degrader and its involvement in corrosion of carbon steel API 5LX was deciphered.
- Biofilm play key role in acceleration of the MIC.
- Understanding of the diversity of bacterial species involved in corrosion will be useful for the development of a new approach to control MIC.

GRAPHICAL ABSTRACT



Characterization of hydrocarbon degrading bacteria isolated from Indian crude oil reservoir and their influence on biocorrosion of carbon steel API 5LX

Punniyakotti Parthipan^{a,b}, Punniyakotti Elumalai^a, Yen Peng Ting^c, Pattanathu K.S.M. Rahman^d, Aruliah Rajasekar^{a*}

^aEnvironmental Molecular Microbiology Research Laboratory, Department of Biotechnology, Thiruvalluvar University, Serkkadu, Vellore, Tamil Nadu, India 632 115.

^bElectrochemical Energy Research Lab, Centre for Nanoscience and Technology, Pondicherry University, Puducherry, India 605 014,

^cDepartment of Chemical and Biomolecular Engineering, National University of Singapore, 4Engineering Drive 4, Singapore 117 576.

^dChemical and Bioprocess Engineering Group, School of Science and Technology, University of Teesside, Middlesbrough TS13BA Tees Valley, UK.

*Corresponding author

A. Rajasekar

Tel. +91 8675265635; fax: 04162274748

Email: rajasekargood@gmail.com

ABSTRACT

The role of biosurfactants producing hydrocarbon-degrading bacteria (HDB) on biodegradation and bio-corrosion was evaluated. Biodegradation efficiency (BE) of *Streptomyces parvus* B7 was found to be 82% when compared to other bacteria. Increased production of biosurfactants directly influences the rate of crude oil BE. Corrosion of carbon steel was found to be more severe in mixed bacterial consortia (1.493 ± 0.015 mm/y). X-ray diffraction confirmed the presence of high intensity of ferric oxide (Fe_2O_3), iron oxide (Fe_3O_4), manganese oxide (Mn_3O_4), and manganese dioxide (MnO_2) in corrosion product of mixed bacterial system. Biofilm formation was assist to pit formation on the carbon steel surface and it was evidenced from the atomic force microscopy (AFM) and scanning electron microscopy (SEM) analysis. Corrosion current was increased in the presence of mixed consortia $1.6 \pm 0.2 \times 10^{-3}$ A/cm², compared to abiotic control $1.2 \pm 0.15 \times 10^{-4}$ A/cm², this values were well supported with charge transfer values and these observations confirmed that mixed bacterial consortia play key role in the corrosion of carbon steel. This is the first report to show degradation of crude oil by *Streptomyces parvus* B7 and its effects on the corrosion of carbon steel in oil reservoir.

Keywords: Biocorrosion; Carbon steel; Biofilm; Biodegradation; Electrochemical impedance spectroscopy

1. Introduction

Biodegradation is a naturally occurring process in polluted environment where microorganisms take part as a pivotal portion. Consequently, it is very essential to comprehend the activities of microorganisms which are responsible for the biodegradation of compounds, including crude oil hydrocarbon (Hassanshahian, 2014; Parthipan et al., 2017a,b). In general, crude oil biodegradation affects the physiochemical nature of petroleum, follow-on in a drop off of hydrocarbon level and an increase in viscosity, acidity, sulphur content and oil density, which in turns lead to negative financial outcomes for the oil production industry and the refining process (Roling, 2003; Tsesmetzis et al., 2016; Parthipan et al., 2017a,b). Water flooding is commonly used to increase the reservoir pressure for improving oil recovery. This process also introduces microorganisms as well as chemicals which act as micronutrients, encouraging microbial proliferation, and which can lead to reservoir souring (Youssef et al., 2009). The prevention of entry of microorganism in fuel and crude oils both in oilfields after drilling, and in storage tanks is challenging. Both aerobic/anaerobic microorganisms form microbial colonies in the oil pipelines as well as in oil and fuel storage equipments. Complex microbial groups, including hydrocarbon utilizing microbes and anaerobic microorganisms, use metabolites synthesized by other microorganisms for their growth.

High/low molecular weight hydrocarbons present in crude oil, depend upon the physiochemical properties of the oil field (Uzoigwe et al., 2015; Pi et al., 2016; Parthipan et al., 2017b). The ability of microorganisms to use hydrocarbons as carbon source has drawn considerable attention presently (Laczi et al., 2015; Chen et al., 2017). Crude oil is naturally hydrophobic compounds that usually need to be softened earlier to their utilization by microorganisms (Radhika et al., 2014; Liu et al., 2014; Parthipan et al., 2017a). While growing on hydrocarbons, many microorganisms produce emulsifiers with the purpose of

increasing hydrocarbons bioavailability and consequent degradation by the microbial consortium (Radhika et al., 2014; Uzoigwe et al., 2015). Emulsification is an important process that can influence the density of crude oil. Emulsifier contains hydrophilic head along with hydrophobic tail in nature (Bharali et al., 2011). In general, it is recognized that microbes grow on hydrocarbons and other substrate and leads to production of biosurfactants, which emulsify substrates and enable their transport into cells. Biosurfactants are surface-active agents and are complex biomolecules (which include fatty acids, peptides and polysaccharides) which have the aptitude to reduce surface tension (Youssef et al., 2009; Das and Ma, 2013; Parthipan et al., 2017b). This is achieved by solubilising fatty acids that coexist in the crude oil, consequently directs to efficient utilization of hydrocarbon by microorganisms. Biosurfactants have several physiological roles and provide environmental advantages to their synthesizers. These are originating in diverse environment, while more in location that are highly contaminated with pollutants, such as oil sludge, petroleum waste, than in un-contaminated environments (Hassanshahian, 2014). They play a critical role in bioremediation by boosting their bioavailability through the circulation of pollutants into the aqueous phase. Moreover, they may also manipulate the competence of the microorganisms applied for bioremediation (Kavitha et al., 2014).

Microbiologically induced corrosion (MIC) is an biological process, where microorganisms instigate, assist, or step up the corrosion mechanism over the surface of metal and leading to metal deterioration (Jan-Roblero et al., 2004; Rajasekar et al., 2007a; Machuca et al., 2014; Parthipan et al., 2017c; Wade et al., 2017). Leakage of crude oil due to the internal corrosion on transporting pipelines has been well reported globally. For instance important pipeline crashes (Prudhoe Bay, AK) (Brouwer et al., 2006; Lenhart et al., 2014) suggest that microbial corrosion may be a causative factor. Microbiological activity in oil reservoir leads to fuel contamination, unacceptable level of turbidity, metal corrosion in

103 pipelines, storage tanks and souring of oil products (Hamilton, 1985; Rajasekar et al., 2010).
104 Besides, water can as well stratify at the substructure of oil pipeline if the oil rapidity is not
105 adequate to entrain water and brush it through the transporting pipeline (Rajasekar et al.,
106 2007). The occurrence of microbes is the important thing liable to the corrosion concern in oil
107 industries (Lenhart et al., 2014; Machuca et al., 2014).

108 Biocorrosion is one of vital characteristic of pipeline letdown, and also it is significant
109 factor for the increases in the process and repairs cost in the oil and gas industries (Lee et al.,
110 2010; Suflita et al., 2012). In general, nearly 40% of pipeline problems in the oil and gas
111 industries originate from microbial activities (Rajasekar et al., 2007b). Biocorrosion has
112 synergistic effect among the metal surface, corrosive medium and rust products created in
113 biofilm over the surfaces of metal (Javaherdashti et al., 2006; Machuca et al., 2016; Eckert
114 and Skovhus, 2016). Extracellular polymeric substances (EPS) contribute a key function in
115 formation of biofilm on metallic/non-metallic surfaces (Little et al., 1991; Little and Lee,
116 2007; Reyes et al., 2008). Biofilm development begins with affections of microbes on firm
117 exterior, and higher emission of EPS metabolites show the way to the expansion of a thicker
118 biofilm and further spreading of individual cell which yet over again commence to form new
119 biofilms on near metal surfaces (Rajasekar et al., 2007a; Forte Giacobone et al., 2011;
120 AlAbbas et al., 2013).

121 The intention of the current investigation is to identify mesophilic crude oil
122 hydrocarbon degrading bacteria isolated from crude oil reservoir, and to elucidate their effect
123 on carbon steel corrosion. Bacterial isolates were screened for biosurfactant production to
124 understand their role in crude oil degradation. Additionally, impact of the crude oil degrading
125 bacteria on biocorrosion of carbon steel was examined.

126 2. Materials and methods

2.1. Sample collection

Crude oil and produced water samples were collected from the crude oil reservoir, Karaikal, India (latitude: 10.7694 and longitude: 79.6155) using sterilized sample containers. The temperature at the sampling point ranged from 30 to 70 °C and the depth of the reservoir was 1200 to 2000 m. The collected samples were transported immediately to the environmental molecular microbiology research laboratory, Thiruvalluvar University, Vellore, India. Samples were sustained at 4 °C until further studies.

2.2. Isolation and molecular identification of bacteria

Bushnell-Haas medium (BH) comprising: 0.2 g L⁻¹ MgSO₄, 0.02 g L⁻¹ CaCl₂, 1.0 g L⁻¹ KH₂PO₄, 1.0 g L⁻¹ K₂HPO₄, 1.0 g L⁻¹ (NH₄)(NO₃), 0.5 g L⁻¹ FeCl₃, and 15.0 g L⁻¹ agar (Hi-Media, Mumbai, India) was utilized to isolate hydrocarbon degrading bacteria. Enumeration procedure was followed as previously described in Rajasekar et al. (2010). Sterile crude oil (1% v/v) was added as the sole carbon source, for the enumeration and isolation of crude oil degrading bacteria. The samples (both produced water and crude oil) were successively diluted up to 10⁻⁶ dilution and 1 mL of every dilution was plated in triplicate by pour plate technique. The plates were kept at 37 °C for 24 – 48 h, following which the bacterial colonies were calculated and dissimilar (morphology and appearance) colonies were picked from each plate. The picked colonies were further purified using BH plates (with 1% crude oil as carbon source) by streak plate method and the pure isolates thus obtained were maintained in BH slants (with crude oil) for additional examination. Selected dissimilar isolates were further screened for the following biochemical characterizations: Gram staining, methyl red, motility, indole production, Voges-Proskauer, citrate, catalase, carbohydrate fermentation, oxidase, gelatine, starch and lipid hydrolysis test as described in Holt et al. (1994). Further

strains were used for molecular identification up to species level by 16S rRNA gene sequencing. DNA of selected isolates was extracted as described by Ausubel et al. (1988). The 16S rRNA gene was amplified using primers (27F/1492R) and amplifications and sequencing were the same as described in Rajasekar et al. (2010).

2.3. Screening for biosurfactant production and characterization

Selected bacteria were screened for biosurfactant production as described in Parthipan et al. (2017a). Biosurfactants production was confirmed using a series of screening assays including drop collapse test (Jain et al., 1991), oil displacement method (with crude oil), emulsification activity (with hexadecane) (Hassanshahian, 2014; Padmavathi and Pandian, 2014) and hemolytic test (Hassanshahian, 2014). All the assays were performed in triplicate and sterile distilled water was used as control. Biosurfactant extracted from strain B7 was used for surface tension measurement as described by Sakthipriya et al. (2015). Further extracted biosurfactant was characterized using gas chromatography and mass spectrometry (GC-MS) as described in Parthipan et al. (2017a). Functional groups were confirmed using fourier transform infrared spectrometry (FTIR, model: Perkin–Elmer, Nicolet Nexus – 470). Briefly, obtained biosurfactant was mixed with the KBr in the ratio of 1:100 and the prepared pellet was preset in the sample holder, and analyzes was performed in the mid IR region 400–4000 cm^{-1} (Parthipan et al., 2017a).

2.4. Crude oil biodegradation

Before the biodegradation studies were performed, the identified isolates were pre-grown overnight at 37 °C with crude oil as substrate. Degradation of crude oil was evaluated

following the protocol as mentioned by Rahman et al. (2002). Pre-grown individual bacterial culture and mixed consortia (2.1×10^4 CFU mL⁻¹) were transferred in a 250 mL Erlenmeyer flask, each included 100 mL of BH broth added with 1% (v/v) sterile crude oil as sole carbon source. An un-inoculated flask was also used to examine the abiotic loss of crude oil hydrocarbon. All the flasks were kept at 37 °C for 20 days at 200 rpm. All the testing were carried out in triplicate. A set of flasks were retrieved at 2 days interval, and utilized for the bacterial count in standard plate-count agar (Hi-Media, Mumbai, India) by the plate counting technique. At the end of the incubation period, biodegradation of crude oil hydrocarbons was examined using GC-MS and FT-IR as described in Parthipan et al. (2017a).

2.5. Bio-corrosion studies

MIC of carbon steel was investigated as previously described by Rajasekar et al. (2010), with minor modifications by using crude oil instead of diesel. Carbon steel API 5LX for weight loss studies and electrochemical studies was prepared as described in Parthipan et al. (2017c). The control system consisted of coupons placed in a 1 L Erlenmeyer flask with 500 mL crude oil including 20% (v/v) sterile produced water. The experimental system was similar to the control, except that the flask was inoculated with 2 mL of mixed bacterial consortia including *B. pumilus* B1, *B. subtilis* B5, *B. megaterium* B6 and *S. parvus* B7 (each 10^6 CFU mL⁻¹). Triplicates were performed for each system. Metal coupons were retrieved with two days of interval until the 20th day of incubation and total viable count was observed using formed biofilm to monitor the bacterial growth through the plate count method, using standard plate-count agar (Hi-Media, Mumbai, India). In addition the biofilm samples was also utilized for identifying living/dead cells at two days interval using dual staining of fluoresce in isothiocyanate and propidium iodide as described in Dhandapani et al. (2012).

Electrochemical impedance spectroscopy (EIS) coupons recovered from both systems were used for EIS studies. The corrosive medium as collected from the both systems was used as the electrolyte solution for EIS studies as described in Parthipan et al. (2017c).

2.6. Surface analysis

After the weight loss experiment, the coupons were recovered, and the rust materials were carefully detached for subsequent surface analysis. All the coupons were cleaned using Clark solution as prescribed in Rajasekar et al. (2011) and subjected to the further analysis. For surface analysis, metal coupons were prepared as described in Rajasekar et al. (2017), further scanning electron microscopy (JEOL JSM-5600LV) with 15 kV beam of electrical energy was used to visualize the biofilm morphology. Final weight of the coupons were used to measure the corrosion rates as suggested by the American Society for Testing and Materials, using this formula: $CR = (K \times W) / (A \times T \times D)$, where, K = a constant (8.76×10^4), W = mass loss in grams, A = area in cm^2 , T = exposure time in hours and D = density in g/cm^3 (Rajasekar et al., 2017). In addition to SEM, surface pits were also studied using atomic force microscopy (AFM) (Rajasekar et al., 2008). The standard deviations for all systems were also calculated. Corrosion products collected from both bio-corrosion systems was analyzed using X-ray diffractometer (XRD) as described in Parthipan et al. (2017c). FT-IR was used to find out the character of oxides/functional material obtained from both biotic/abiotic systems (Rajasekar et al., 2007a).

2.7. Nucleotide sequence accession number

The sequence used in current study was allocated the accession numbers KP895567-KP895570 by the National Centre for Biotechnology Information (NCBI). *Streptomyces parvus* B7 strain has been deposited in the Deutsche Sammlung von Mikroorganismen und Zellkulturen depository (DSMZ-Germany) with the code DSM 101525, and in the National Collection of Industrial Microorganisms, CSIR - National Chemical Laboratory (NCIM-NCL) – Pune, India, under the number of NCIM- 5587.

3. Results

3.1. Molecular identification of the isolates

The physiochemical properties of produced water are presented in Table 1. The produced water included with considerably high amount of chloride, 4-5% carbonate, sulphate, as well as trace amounts of other elements. Preliminary biochemical identification revealed the identity of crude oil degrading strains (CDSs) as belonging to the Gram positive genera only (Table 2). The phylogenetic relationship (*Firmicutes* and *Actinobacteria*) was verified by analyzing each relevant species predicted by the categorization and taxonomic hierarchy, and completed with the NCBI and Ribosomal Database Project-II Release 10. Phylogenetic tree was assembled using neighbor-joining method for the isolates (Fig. 1) to evaluate the relations amongst the bacteria with interrelated species from the GenBank database. 16S rRNA sequence alignment analysis revealed more than 99% similarity between *Bacillus pumilus* B1, *B. subtilis* B5, *B. megaterium* B6 and *Streptomyces parvus* B7.

3.2. Analysis of biosurfactant production

The four bacterial isolates *B. pumilus* B1, *B. megaterium* B6 and *S. parvus* B7 showed a positive zone of clearance in the hemolytic test, while *S. parvus* B7 and *B. pumilus* B1 displayed higher emulsification activity compared to *B. subtilis* B5 and *B. megaterium* B6 (Table 3). The all four strains were conferring positive for both drop collapse activity and oil spreading assay. These observations established the biosurfactant presences in the culture broth. The oil displacement activity was directly relative to the occurrence of the biosurfactant level in the solution. The emulsion index (E24) of the isolates with hexadecane ranged from 23 to 46%. This emulsification activity established unambiguously the production of biosurfactants by the isolates. Biosurfactant produced by strain *S. parvus* B7 reduces surface tension about $22.6 \pm 0.2 \text{ mN m}^{-1}$ from $72.42 \pm 0.2 \text{ mN m}^{-1}$.

Gas chromatography analysis revealed that major components present in the extracts were fatty acids only. *S. parvus* B7 (Fig. 2a) biosurfactant contained following fatty acids: n-hexadecanoic acid ($\text{C}_{16}\text{H}_{32}\text{O}_2$) (32.49%) (Fig. 2b), oleic acid or octadecanoic acid ($\text{C}_{18}\text{H}_{34}\text{O}_2$) (Davila et al., 1992) (40.33%) (Fig. 2c) and octadecanoic acid, methyl ester ($\text{C}_{19}\text{H}_{38}\text{O}_2$) (Figure 2d) accounting for 17% of the whole peaks present in the GC spectra. Hexanedioic acid, bis (2-ethylhexyl) ester ($\text{C}_{22}\text{H}_{42}\text{O}_4$) (Hien et al., 2013) was present in the remaining strains such as *B. pumilus* B1 (Fig. S1), *B. subtilis* B5 (Fig. S2) and *B. megaterium* B6 (Fig. S3). In addition palmitic acid ($\text{C}_{16}\text{H}_{32}\text{O}_2$) (Davila et al., 1992) also presents in *B. pumilus* B1 and palmitic acid, methyl ester ($\text{C}_{17}\text{H}_{34}\text{O}_2$) was present in *B. megaterium* B6. FT-IR analysis of the biosurfactant produced by *S. parvus* B7 (Fig. 3) confirmed it was a fatty acid in nature. FT-IR spectra revealed a peak at 599 cm^{-1} arising from C–I (Carbon–Iodine) bond. The peak at 638 cm^{-1} confirms the presence of C–Br. The peak at 3116 cm^{-1} represents the cumulated system $\text{R}_2\text{C}=\text{N}=\text{N}$ in the sample. An absorption band at 976 cm^{-1} was found to be stretching of $\text{RCH}=\text{CH}_2$ which indicating the presence of alkenes. The wave numbers 3560, 2308 and 2390 cm^{-1} reveals the stretching of N–H group. The transmittance at 1405 cm^{-1} was caused by

the aliphatic chain of the C–H group. Intense stretching peaks at 1171 and 1645 cm^{-1} indicates the presence of R-NO₂ groups. The presence of these chemical groups determinedly revealed that biosurfactant was fatty acid in nature (Sarafin et al., 2014).

3.3. Crude oil degradation analysis

Fig. 4 shows the growth curve of the isolates in being there of crude oil as sole energy source. Crude oil utilization capability of the bacterial isolates were constantly observed and noted that after the inoculation of isolates, clear BH medium turns into turbid within the 2nd day of incubation. The turbidity of the growth medium was increased constantly with increasing incubation period. The maximum growth rate was recorded between 10-14th day of incubation and further days the growth rate was slowly decreased. The GC–MS chromatogram of crude oil biodegradation is exposed in Fig. 5 and Table 4 shows the biodegradation efficiency of crude oil. The degradation of crude oil by *B. pumilus* B1, *B. subtilis* B5, *B. megaterium* B6, and *S. parvus* B7 strains showed biodegradation efficiency (BE) of about 66 %, 55 %, 52 %, and 82 % respectively. Mixed bacterial consortia (*B. pumilus* B1, *B. subtilis* B5, *B. megaterium* B6 and *S. parvus* B7) showed a maximum BE of 90% after 20 days of incubation. More precisely, *S. parvus* B7 showed a 95% BE in regards to C₁₀-C₂₀, while strains *B. pumilus* B1, *B. subtilis* B5, and *B. megaterium* B6 had a 100% BE for C₁₀-C₁₁. At the same time, degradation of other n-alkanes (C₁₂-C₂₀) was weak (about 40-65%), even after 20 days of incubation. *S. parvus* B7 showed a maximum BE of 82% and reached a population size of 2.92 x 10⁵ CFU mL⁻¹. This observation suggests that *S. parvus* B7 has a high aptitude to utilize all molecular weight crude oil hydrocarbons. Besides *S. parvus* B7, mixed bacterial consortia also have high prospective to remove the broad range of hydrocarbons present in the crude oil.

The FT-IR spectra of crude oil, in the abiotic control system, showed characteristic bands of C–H aliphatic stretch, C=C stretch in aromatic nuclei, C-H bend alkanes, C–N stretch aliphatic amines and N–H wag of 1°, 2° amines (Fig. 6a). The FT-IR spectra of crude in the presence of CDSs *B. pumilus* B1, *B. subtilis* B5, *B. megaterium* B6, *S. parvus* B7 and mixed consortia, shows decreased bands intensity (Fig. 6b-f). Absence of aliphatic and amine peaks at 1092 cm⁻¹ and 902 cm⁻¹ was due to the degradation of respective hydrocarbons.

3.4. Bio-corrosion studies

3.4.1. Weight loss studies

The carbon steel corrosion rate in different bio-corrosion systems is presented in Table 5. The abiotic control system displayed a weight loss of 40 ± 3 mg, whereas the presence of mixed consortia increased the weight loss up to 201 ± 3 mg (Table 5). The corresponding corrosion rates (0.297 ± 0.020 mm/y and 1.493 ± 0.015 mm/y) were considered high or severe respectively (Powell, 2015). Fig. 7 showed the growth pattern of the mixed consortia in the occurrence of crude oil as sole carbon source in the corrosive medium. Maximum growth (10⁶) was reached at 5th day of the incubation and cell numbers was decreased slowly from 7th day of the incubation. Growth pattern confirmed that the active growth of the CDSs in the bio-corrosion system and no countable cells was found in the abiotic system. Fig. 8 showed the epi-fluorescence microscopic observations of the bacterial cells collected from biofilm. From this figure, the presence of green fluorescence specified the existence of viable bacterial cells (Fig. 8a-c). In later stages at 8th and 10th day of incubation some of the dead cells were observed and it was specified by the presence of the

red fluorescent spots in the Fig. 8d&e. This observation confirms that mixed consortia were active throughout the biocorrosion study periods.

3.4.2. Electrochemical impedance spectroscopy

Fig. 9a shows the potentiodynamic polarization curves for carbon steel API 5LX in abiotic control and mixed consortia inoculated systems. The polarization values such as corrosion potential (E_{corr}), the corrosion current density (I_{corr}), and the anodic tafel slope (β_a) and cathodic tafel slope (β_c) Tafel values were stated in Table 6. From the polarization information it can be observed that the I_{corr} was increased in the existence of mixed consortia $1.6 \pm 0.2 \times 10^{-3} \text{ A/cm}^2$, compared to abiotic control $1.2 \pm 0.15 \times 10^{-4} \text{ A/cm}^2$. Similarly both β_c and β_a of the mixed consortia systems were increased in comparison with the abiotic system.

Fig. 9b demonstrates the electrochemical impedance data for the carbon steel API 5LX in different corrosion systems. The electron transfer function is thus represented by an equivalent circuit (Fig. 9b inside), which was used for the stimulation of impedance values for both corrosion systems. The impedance parameters such as charge transfer values (R_{ct}), solution resistance (R_s) and biofilm resistance (R_b) values of the both systems were shown in Table 6. The higher values of R_{ct} was recorded in the abiotic system ($21.3 \pm 1 \text{ } \Omega \cdot \text{cm}^2$), compared to mixed consortia ($7.7 \pm 0.8 \text{ } \Omega \cdot \text{cm}^2$). This could possibly be attributed to the thin biofilm-iron oxide deposit on the carbon steel surface, in the control system, which enhances the corrosion.

3.4.3. Surface analyses

The micrographs of bacterial biofilm (Fig. 10a & Fig. 10b) revealed that these CDSs have the ability to form dense micro colonies with accumulated metabolites (EPS). Corrosion caused by these CDSs was evaluated by examining the pits on the surface of carbon steel, following the exclusion of the biofilm and corrosion products from the coupons. Examination of the metals under SEM revealed smooth surface in the abiotic control system (Fig. 11a), whereas pitting type corrosion was observed on the surface of carbon steel in the mixed consortia system (Fig. 11b). Further the pits were confirmed by AFM analysis, 2D and 3D images of the abiotic control coupon and mixed consortia coupons along with cross-sectional analysis of the coupons are shown in Fig. 12a & b. Bacterial strains accelerated the pitting corrosion on carbon steel API 5LX surface. The micro-pitting encouraged by bacterial strains looks greater in comparison with that uninoculated control system, as revealed by the standard AFM software on the pitted areas. Based on this analysis, depth of pits accelerated by bacterial strains as range between -500 to -1000 nm compared to control coupons (below -3nm). The depth of pits proliferates with time and lead to deeper pits on carbon steel surface. In aerobic corrosion processes, oxidation takes place at the cathodic positions to formation of hydroxides. Aerobic corrosion takes place while oxygen is retained from the surface of metal through microorganisms. Consequently pit formation or corrosion reactions occur rapidly beneath the biofilm by aerobic corrosive bacterial strains (Parthipan et al., 2017d).

Fig. 13a and 13b show the XRD spectra of the corrosion product collected during the bio-corrosion studies. Iron oxide hydroxide ($\text{FeO}(\text{OH})$), ferrous hydroxide ($\text{Fe}(\text{OH})_2$) manganese dioxide (MnO_2) and ferrous chloride (FeCl_2) were detected in the control system (Fig. 13a). More intense peaks of ferric oxide (Fe_2O_3), iron oxide (Fe_3O_4), manganese oxide (Mn_3O_4), and manganese dioxide (MnO_2) were instead found in the mixed consortia system (Fig. 13b) (Rajasekar et al. 2007c; Parthipan et al., 2017c&d).

The FT-IR analysis of the rust products collected from different corrosion systems are shown in Fig. 14. In both control and experimental systems, broad bands were found at 3427 and 3435 cm^{-1} , and were endorsed to the OH group. In the control system, peaks ranged from 2924 to 2850 cm^{-1} , and were consigned to $-\text{CH}-$ stretching of aliphatic hydrocarbons present in the crude oil. The peak at 1628 cm^{-1} is owing to COO^- (carboxylate anion) and the one at 602 cm^{-1} specifies the stretch of iron oxides (FeO). The peak at 1633 cm^{-1} is owing to $\text{C}=\text{O}$ (stretch (amide I) related to proteins) and is attributed to the formation of bacterial exopolymer secretion (EPS) (Badireddy et al., 2010). New peaks were noticed at 1365 cm^{-1} representative to the existence of $\text{C}-\text{H}$ alkanes on the metal surface. A peak at 1024 cm^{-1} identifies the stretching intended for $-\text{C}-\text{O}-$ stretch for $-\text{C}-\text{O}-\text{C}-$ group. One peak at 877 cm^{-1} specifies the existence of FeO whereas the peak at 568 cm^{-1} was attributed to $\text{C}-\text{Cl}$ bond (Rajasekar et al., 2007a).

4. Discussion

The produced water samples collected from an Indian crude oil reservoir contains considerable level of chloride, carbonate and sulphate. These chemicals, together with the crude oil as carbon source, support microorganisms in the oil reservoir. The ability of Gram positive bacteria (bacilli) to form endospores is a vital adaptation machinery among the microorganisms living in extremes and unstable environments, such as those with high temperature, pressure, marine sediments, semi-arid circumstances, and with hot summers (Shimura et al., 1999). The growth of microorganisms in crude oil is often linked to the production of biosurfactants (Rajasekar et al., 2008). Production of biosurfactant allows microorganisms to uptake the hydrocarbons, with a positive effect on their growth, which has significant implications in the oil reservoir (Maruthamuthu et al., 2005; Parthipan et al.

2017a). The surface reducing nature of the strain B7 confirms that produced biosurfactant has the capabilities to reduce the surface tension of the medium in presence of the crude oil as substrate and it will enhance the solubility of the crude oil (Sakthipriya et al. 2015).

While the CDSs used throughout this study were isolated from a crude oil reservoir, they can also easily adapt to, and survive in the oil-contaminated aqueous medium. All the bacterial strains produced different biosurfactant compounds which are classified as fatty acid in nature.

The bacterial isolates showed luxuriant growth in crude oil by using it as carbon source; they also exhibited efficient crude oil degradation corresponding to an increase in cell population. The GC-MS spectra (Fig. 5) confirm that the bacterial strains have the capability to utilize crude oil hydrocarbons. During degradation, the cationic moieties of the biosurfactants have attraction towards negatively charged bacterial membrane in connection with crude oil. The hydrophobic part of the biosurfactant is believed to allow the peptides to sliver and permeate into the membrane (Mulligan and Gibbs, 2004).

From the utilization of low molecular weight hydrocarbons, bacteria produce biosurfactants, which assist in the crude oil solubilization and bacterial growth. Cell growth was then promoted by the 'degraded' oil products and additional emulsifying agents were then produced (Radhika et al., 2014). In the present work, synthesise of the biosurfactant by bacterial strains leads to highest biodegradation efficiency of hydrocarbon by increasing their solubility. Thavasi et al. (2011) described that degradation of crude oil by *Corynebacterium kutscheri*, *B. megaterium*, and *Pseudomonas aeruginosa* was enhanced by the production and action of biosurfactants. The GC spectra analysis of the degraded residual compounds confirmed that all the bacterial strains are capable of breaking down the complex hydrocarbons found in the crude oil. Rajasekar et al. (2007a) reported the ability of *Serratia marcescens* to degrade diesel/naphtha hydrocarbon.

EIS measurements were considered to elucidate the consequence of bacterial strains on biocorrosion of carbon steel API 5LX. EIS is a non-destructive method for distinguishing electrochemical process at metal/biofilm interfaces and observing development of corrosion products and biofilms during microbial corrosion. Potentiodynamic polarization observations confirmed that the corrosion current and anodic/cathodic tafel slope were enhanced in bacterial system. This finding further confirmed that these bacterial strains increased the corrosion rate (1.493 ± 0.015 mm/y) of carbon steel through inducing cathodic reactions. In a biofilm, electrons are accepted from metal surface, creating an alleyway of electron flow from carbon steel (anode) to the collective electron acceptor oxygen (cathode); and as a result accelerated bio-corrosion (Tsai and Chou, 2000).

Impedance observations as well as confirmed bacterial attachment are corrosive nature that leads to the decreases of corrosion resistance. Lower impedance value in the presence of mixed consortia was due to the weakening of protective effects. The presence of biofilm and prevalence of bacterial metabolic activities can considerably involve in the decline of passivity while bacterial metabolites and chloride ions accumulate at metal surface. Consequently, the impedance parameters decreased over the period of exposure.

Bacterial biofilm play crucial role in the pit formation on carbon steel surface. Similar observations were observed recently by Machuca et al. (2016). There is no considerable pit was observed in carbon steel immersed in the abiotic control system, it could be due to the very less corrosiveness in the absence of bacterial consortia. These results were well supported by the SEM observations. Bacterial attachment and the subsequent biofilm development are the decisive steps in biological mediated metal deterioration (Parthipan et al., 2017d). From the epi-fluorescence microscopy analysis the biofilm formation was higher with active cells throughout the incubation period of the biocorrosion study (Fig.8a-c). In the current study, destructive ions, such as chloride, attached over the metal surface with the

CDSs and induced corrosion. Besides, the existence of bacteria on surface of carbon steel can encourage rigorous attack because of the alterations in the microchemistry of the metal surface modified by bacterial metabolism (Tsai and Chou, 2000).

The presence of Fe_2O_3 in the corrosion product confirms that the CDSs accelerated the corrosion of carbon steel API 5LX (Hamilton, 1985). These results revealed the presence of high intensity corrosion products including Fe_2O_3 , Fe_3O_4 , Mn_3O_4 , and MnO_2 , confirming the role of mixed bacterial consortia in iron/manganese oxidations, which accelerates the corrosion process (Parthipan et al., 2017c). Block/grey rust product was observed over the carbon steel in the mixed consortia system, it could be due to the occurrence of magnetite in the rust products as identified in XRD analysis.

Degraded hydrocarbons in crude oil promote the development of bacteria and augment the rust formation (Lenhart et al., 2014; Aktas et al., 2017). Also degraded hydrocarbons enhance the development of ferric oxide. Consequently, bacteria accelerate the corrosion reaction by forming Fe_2O_3 . The occurrence of inorganic substances such as ferric, in rust product, indicate that mixed consortia accelerate the development of ferric/manganese complex products (Rajasekar et al., 2007b, 2010). Similar results were previously reported by Rajasekar et al. (2005), indicating that a number of crude oil consuming bacteria oxidize the Fe^{2+} to Fe^{3+} by addition of O_2 commencing from the biodegraded compounds, leading to the formation of organic complex. Because ferric has a higher attraction for O_2 , it removes O_2 from the biodegraded product and boosts the development of Fe_2O_3 and enhances the corrosion process (Rajasekar et al., 2010)

4.1. Biocorrosion mechanism

The isolated CDSs identified here belong to the *Bacillaceae* and *Streptomycetaceae* families. These isolates consume hydrocarbon with a wide range of molecular weight. Among the identified species, *S. parvus* B7 displayed a maximum BE of 82% for hydrocarbons, including light and heavy hydrocarbons found in the crude oil (Fig. 5 and Fig. 6). Biosurfactant involved an exceptionally important function in enhancing the degradation of crude oil. In our study, the isolate *S. parvus* B7 acts as good crude oil degrader due to the production of biosurfactant and its higher emulsification abilities. These strains are facultative anaerobes, and biochemical tests confirmed that they express both cytochrome oxidase and catalase enzymes. All strains also express catalase, which neutralize the toxicity of H_2O_2 into H_2O and O_2 . These strains then utilize oxygen and hydrogen in the respiration process. O_2 radicals, formed by bacterial metabolism, combined with the nearby iron atom present on surface of the metal, form a superoxide surface anion radical. Eventually, the metal surface anion reacts with H_2O , which directs the oxidation of Fe^{2+} to Fe_2O_3 as rust compounds, besides the hydroxide anion (Fig. 13 and Fig. 14) (Rajasekar et al., 2011). This observation corroborates the work of Lenhart et al. (2014) who demonstrated that microorganisms utilise the hydrocarbon and ferrous ion as organic and inorganic sources respectively and thus accelerate the corrosion of carbon steel in crude oil reservoir (Ching et al., 2016; Aktas et al., 2017). In general, the results obtained in this study support the theory that the MIC of carbon steel takes place through the contribution of Fe_2O_3 , which is a consequence of degradation of crude oil hydrocarbons.

Nowadays, addition of inhibitors/biocides is extensively used for managing corrosion in the oil industry. It is crucial to select appropriate and effective inhibitor/biocide, as many microorganisms present in oil and other petroleum products are capable of degrading these compounds and utilize them for their development and growth, hence unwittingly promoting corrosion as well (Maruthamuthu et al., 2005). It is therefore essential to have a basic

understanding of the physiology of bacterial communities present in crude oil reservoir, which will help selecting a suitable inhibitor/biocide for the control of MIC in crude oil reservoir.

5. Conclusions

To conclude, the isolate *S. parvus* B7 showed a BE of crude oil of up to 82%, aided by the high biosurfactant production. Mixed bacterial consortia converts Fe^{2+} to Fe_2O_3 by adding oxygen during the degradation process, thus forming iron oxide complexes (rust) on carbon steel, the maximum corrosion rate was recorded in the mixed consortia system (1.493 ± 0.015 mm/y). Biofilm formation assisted pit formation on the carbon steel surface and it was evidenced from the SEM and AFM analysis. Corrosion current was increased in the presence of mixed consortia this observation confirmed that mixed bacterial consortia play key role in the corrosion of carbon steel. These observations enlarge the understanding of bacterial communities related to biocorrosion of carbon steel as well as distinguish the corrosive properties of bacteria belonging to the *Streptomycetaceae* family.

Acknowledgments

A. Rajasekar is thankful to the Department of Biotechnology (Government of India) for the award of the Ramalingaswami re-entry Fellowship (BT/RLF/Re-entry/17/2012), Department of Science and Technology for the young scientist award (SB/YS/LS-40/2013) and Science and Engineering Research Board (SERB), Department of Science and Technology (DST), Government of India (EEQ/2016/000449). Dr. P. Parthipan is acknowledging to the DST-SERB for the financial support (PDF/2017/001134). The authors

also thank Dr. S. Maruthamuthu and Mr. P. Dhandapani CSIR-CECRI for their assistance in GC-MS analysis and related discussions in spectral recordings. Special thanks are due to Mr. Subramanian (technical assistant) in the Central Instrumentation Facility, CSIR-CECRI, Karaikudi for assistance in GC-MS analysis.

Conflicts of interest

The authors declare no competing financial interest.

References

- Aktas, D.F., Sorrell, K.R., Duncan, K.E., Wawrik, B., Callaghan, A.V., Suflita, J.M., 2017. Anaerobic hydrocarbon biodegradation and biocorrosion of carbon steel in marine environments: The impact of different ultra low sulfur diesels and bioaugmentation. *Int. Biodeterior. Biodegrad.* 118, 45-56.
- AlAbbas, F.M., Williamson, C., Bhola, S.M., Spear, J.R., Olson, D.L., Mishra, B., Kakpovbia, A.E., 2013. Influence of sulfate reducing bacterial biofilm on corrosion behavior of low-alloy, high-strength steel (API-5L X80). *Int. Biodeterior. Biodegrad.* 78, 34-42.
- Ausubel, F.M., Brent, R., Kingston, R.E., Moore, D.D., Seidelman, J.G., Struhl, K.E., 1988. *Current protocols in molecular biology*, Wiley, New York.
- Badireddy, A.R., Chellam, S., Gassman, P.L., Engelhard, M.H., Lea, A.S., Rosso K.M., 2010. Role of extracellular polymeric substances in bioflocculation of activated sludge microorganisms under glucose-controlled conditions. *Water Res.* 44, 4505-4516.

545 Bharali, P., Das, S., Konwar, B.K., Thakur, A.J., 2011. Crude biosurfactant from
 546 thermophilic *Alcaligenes faecalis*: Feasibility in petro-spill bioremediation. Int.
 547 Biodeterior. Biodegrad. 65, 682-690.

548 Brouwer, S., Carey, A., Downs, K., Mousemak, J., 2006. BP: pipeline shutdown could last
 549 weeks or months, USA Today [Internet] [cited 2006 Aug 7]. Available from:
 550 http://usatoday30.usatoday.com/news/nation/2006-08-06-alaskan-oil-field_x.htm.

551 Chen, W., Li, J., Sun, X., Min, J., Hu, X., 2017. High efficiency degradation of alkanes and
 552 crude oil by a salt-tolerant bacterium *Dietzia* species CN-3. Int. Biodeterior.
 553 Biodegrad. 118, 110-118.

554 Ching, T.H., Yoza, B.A., Wang, R., Masutani, S., Donachie, S., Hihara, L., Li, Q.X., 2016.
 555 Biodegradation of biodiesel and microbiologically induced corrosion of 1018 steel by
 556 *Moniliella wahieum* Y12. Int. Biodeterior. Biodegrad. 108, 122-126.

557 Das, P., Ma, L.Z., 2013. Pyocyanin pigment assisting biosurfactant-mediated hydrocarbon
 558 emulsification. Int. Biodeterior. Biodegrad. 85, 278-283.

559 Davila, A.M., Marchal, R., Vandecasteele, J.P., 1992. Kinetics and balance of a
 560 fermentation free from product inhibition: sophorose lipid production by *Candida*
 561 *bombicola*. Appl. Microbiol. Biotechnol. 38, 6-11.

562 Dhandapani, P., Maruthamuthu, S., Rajagopal, G., 2012. Bio-mediated synthesis of TiO₂
 563 nanoparticles and its photocatalytic effect on aquatic biofilm. J. Photochem.
 564 Photobiol. B Biol. 110, 43-49.

565 Eckert, R.B., Skovhus, T.L., 2016. Advances in the application of molecular
 566 microbiological methods in the oil and gas industry and links to microbiologically
 567 influenced corrosion. Int. Biodeterior. Biodegrad. doi.10.1016/j.ibiod.2016.11.019.

568 Forte Giacobone, A.F., Rodriguez, S.A., Burkart, A.L., Pizarro, R.A., 2011.
 569 Microbiological induced corrosion of AA 6061 nuclear alloy in highly diluted media
 570 by *Bacillus cereus* RE 10. Int. Biodeterior. Biodegrad. 65, 1161-1168.

571 Hamilton, W.A., 1985. Sulphate-reducing bacteria and anaerobic corrosion. Annu. Rev.
 572 Microbiol. 39, 195–217.

573 Hassanshahian, M., 2014. Isolation and characterization of biosurfactant producing bacteria
 574 from Persian Gulf (Bushehr provenance). Mar. Pollut. Bull. 86, 361-366.

575 Hien, L.T., Yen, N.T., Nga, W.T., 2013. Biosurfactant-producing *Rhodococcus ruber* TD2
 576 isolated from oil polluted water in vung tau coastal zone. Tap. Chi. Sinh. Hoc. 35, 454-
 577 460.

578 Holt, J.G., Kreig, N.R., Sneath, P.H.A., Stanely, J.T., 1994. Bergey's manual of
 579 determinative bacteriology, 9th ed, Williams and Wilkins Publishers, Maryland.

580 Jain, D.K., Collins-Thompson, D.L., Lee, H., Trevors, J.T., 1991. A drop-collapsing test for
 581 screening surfactant producing microorganisms. J. Microbiol. Meth. 13, 271-279.

582 Jan-Roblero, J., Romero, J.M., Amaya, M., Le Borgne, S., 2004. Phylogenetic
 583 characterization of a corrosive consortium isolated from a sour gas pipeline. Appl.
 584 Microbiol. Biotechnol. 64, 862–867.

585 Kavitha, V., Mandal, A.B., Gnanamani, A., 2014. Microbial biosurfactant mediated
 586 removal and/or solubilization of crude oil contamination from soil and aqueous phase:
 587 an approach with *Bacillus licheniformis* MTCC 5514. Int. Biodeterior. Biodegrad. 94,
 588 24-30.

589 Laczi, K., Kis, A., Horvath, B., Maroti, G., Hegedus, B., Perei, K., Rakhely, G., 2015.
 590 Metabolic responses of *Rhodococcus erythropolis* PR4 grown on diesel oil and
 591 various hydrocarbons. Appl. Microbiol. Biotechnol. 99, 9745-9759.

- Lee, J.S., Ray, R.I., Little, B.J., 2010. An assessment of alternative diesel fuels: microbiological contamination and corrosion under storage conditions, *Biofouling* 26, 623-635.
- Lenhart, T.R., Duncan, K.E., Beech, I.B., Sunner, J.A., Smith, W., Bonifay, V., Biri, B., Suflita, J.M., 2014. Identification and characterization of microbial biofilm communities associated with corroded oil pipeline surfaces. *Biofouling* 30, 823-835.
- Little, B., Lee, J.S., 2007. Biofilm formation, in microbiologically influenced corrosion. John Wiley & Sons, Inc, 1-21.
- Little, B., Wagner, P., Mansfeld, F., 1991. Microbiologically influenced corrosion of metals and alloys. *Int. Mat. Rev.* 36, 253-272.
- Liu, H., Yao, J., Yuan, Z., Shang, Y., Chen, H., Wang, F., Masakorala, K., Yu, C., Cai, M., Blake, R.E., Choi, M.M.F., 2014. Isolation and characterization of crude-oil-degrading bacteria from oil-water mixture in Dagang oilfield, China. *Int. Biodeterior. Biodegrad.* 87, 52-59.
- Machuca, L.L., Jeffrey, R., Bailey, S.I., Gubner, R., Watkin, E.L.J., Ginige, M.P., Kaksonen, A.H., Heidersbach, K., 2014. Filtration-UV irradiation as an option for mitigating the risk of microbiologically influenced corrosion of subsea construction alloys in seawater. *Corros. Sci.* 79, 89-99.
- Machuca, L.L., Jeffrey, R., Melchers, R.E., 2016. Microorganisms associated with corrosion of structural steel in diverse atmospheres. *Int. Biodeterior. Biodegrad.* 114, 234-243.
- Maruthamuthu, S., Mohanan, S., Rajasekar, A., Muthukumar, N., Ponmarippan, S., Subramanian, P., Palaniswamy, N., 2005. Role of corrosion inhibitors on bacterial corrosion in petroleum product pipeline. *Indian J. Chem. Technol.* 12, 567-575.

616 Mulligan, C.N., Gibbs, B.F., 2004. Types, production and applications of biosurfactants.
617 Proc. Indian Nat. Sci. Acad. 1, 31–55.

618 Padmavathi, A.R., Pandian, S.K., 2014. Antibiofilm activity of biosurfactant producing
619 coral associated bacteria isolated from Gulf of Mannar. Indian J. Microbiol. 54, 376-
620 382.

621 Parthipan, P., Preetham, E., Machuca, L.L., Rahman, P.K.S.M., Murugan, K., Rajasekar,
622 A., 2017a. Biosurfactant and degradative enzymes mediated crude oil degradation by
623 bacterium *Bacillus subtilis* A1. Front. Microbiol. 8, 193.

624 Parthipan, P., Elumalai, P., Karthikeyan, O.P., Ting, Y.P., Rajasekar, A., 2017b. Review on
625 biodegradation of hydrocarbon and their influence on corrosion of carbon steel with
626 special reference to petroleum industry. J. Environ. Biotechnol. Res. 6(1), 12-33.

627 Parthipan, P., Narenkumar, J., Elumalai, P., Preethi, P.S., Nanthini, A.U.R., Agrawal, A.,
628 Rajasekar, A., 2017c. Neem extract as a green inhibitor for microbiologically
629 influenced corrosion of carbon steel API 5LX in a hypersaline environments. J. Mol.
630 Liq. 240, 121–127.

631 Parthipan, P., Babu, T.G., Anandkumar, B., Rajasekar, A., 2017d. Biocorrosion and its
632 impact on carbon steel API 5LX by *Bacillus subtilis* A1 and *Bacillus cereus* A4
633 isolated from indian crude oil reservoir. J. Bio Tribo Corros. 3, 32.

634 Pi, Y., Meng, L., Bao, M., Sun, P., Lu, J., 2016. Degradation of crude oil and relationship
635 with bacteria and enzymatic activities in laboratory testing. Int. Biodeterior.
636 Biodegrad. 106, 106-116.

637 Powell, D.E., 2015. Internal corrosion monitoring using coupons and ER probes in ‘oil and
638 gas pipelines integrity and safety handbook, edited by. R. Winston Revie, John Wiley
639 & Sons. New Jersey. 495-514.

640 Radhika, C., Jun, Y., Minmin, C., Kanaji, M., Jain, A.K., Martin, M.F.C., 2014. Properties
641 and characterization of biosurfactant in crude oil biodegradation by bacterium
642 *Bacillus methylotrophicus* USTBa. Fuel 122, 140-148.

643 Rahman, K.S.M., Thahira-Rahman, J., Lakshmanaperumalsamy, P., Banat, I.M., 2002.
644 Towards efficient crude oil degradation by a mixed bacterial consortia. Bioresour.
645 Technol. 85, 257-261.

646 Rajasekar, A., Anandkumar, B., Maruthamuthu, S., Ting, Y.P., Rahman, P.K.S.M., 2010.
647 Characterization of corrosive bacterial consortia isolated from petroleum-product-
648 transporting pipelines. Appl. Microbiol. Biotechnol. 85, 175-1188.

649 Rajasekar, A., Balasubramanian, R., Kuma, J.V.M., 2011. Role of hydrocarbon degrading
650 bacteria *Serratia marcescens* ACE2 and *Bacillus cereus* ACE4 on corrosion of carbon
651 steel API 5LX. Ind. Eng. Chem. Res. 50, 10041-10046.

652 Rajasekar, A., Ganesh Babu, T., Karutha Pandian, S., Maruthamuthu, S., Palaniswamy, N.,
653 Rajendran, A., 2007a. Biodegradation and corrosion behavior of manganese oxidizer
654 *Bacillus cereus* ACE4 in diesel transporting pipeline. Corros. Sci. 49, 2694–2710.

655 Rajasekar, A., Ponmariappan, S., Maruthamuthu, S., Palaniswamy, N., 2007b. Bacterial
656 degradation and corrosion of naphtha in transporting pipeline. Curr. Microbiol. 55,
657 374-381.

658 Rajasekar, A., Babu, T.G., Pandian, S.T.K., Maruthamuthu, S., Palaniswamy, N.,
659 Rajendran, A., 2007c. Role of *Serratia marcescens* ACE2 on diesel degradation and
660 its influence on corrosion. J. Ind. Microbiol. Biotechnol. 34, 589-598.

661 Rajasekar, A., Maruthamuthu, S., Muthukumar, N., Mohanan, S., Subramanian, P.,
662 Palaniswamy, N., 2005. Bacterial degradation of naphtha and its influence on
663 corrosion. Corros. Sci. 47, 257-271.

664 Rajasekar, A., Maruthamuthu, S., Ting, Y.P., 2008. Electrochemical behavior of *Serratia*
665 *marcescens* ACE2 on carbon steel API5L-X60 in organic aqueous Phase. Ind. Eng.
666 Chem. Res. 47, 6925-6932.

667 Rajasekar, A., Xiao, W., Sethuraman, M., Parthipan, P., Elumalai, P., 2017. Airborne
668 microorganisms associated with corrosion of structural engineering materials.
669 Environ. Sci. Pollut. Res. 24, 8120–8136.

670 Reyes, A., Letelier, M.V., De la Iglesia, R., Gonzalez, B., Lagos, G., 2008.
671 Microbiologically induced corrosion of copper pipes in low-pH water. Int.
672 Biodeterior. Biodegrad. 61, 135–141.

673 Roling, W., 2003. The microbiology of hydrocarbon degradation in subsurface petroleum
674 reservoirs: perspectives and prospects. Res. Microbiol. 54, 321-328.

675 Sakthipriya, N., Doble, M., Sangwai, J.S., 2015. Action of biosurfactant producing
676 thermophilic *Bacillus subtilis* on waxy crude oil and long chain paraffins. Int.
677 Biodeterior. Biodegrad. 105, 168-177.

678 Sarafin, Y., Donio, M.B.S., Velmurugan, S., Michaelbabu, M., Citarasu, T., 2014. *Kocuria*
679 *marina* BS-15 a biosurfactant producing halophilic bacteria isolated from solar salt
680 works in India, Saudi J. Biol. Sci. 21, 511–519.

681 Shimura, M., Kimbara, K., Nagato, H., Hatta, T., 1999. Isolation and characterization of a
682 thermophilic *Bacillus* sp. JF8 capable of degrading polychlorinated biphenyls and
683 naphthalene. FEMS Microbiol. Lett. 178, 87-93.

684 Suflita, J.M., Aktas, D.F., Oldham, A.L., Perez-Ibarra, B.M., Duncan, K., 2012. Molecular
685 tools to track bacteria responsible for fuel deterioration and microbiologically
686 influenced corrosion. Biofouling 28, 1003-1010.

687 Thavasi, R., Jayalakshmi, S., Ibrahim, M.B., 2011. Effect of biosurfactant and fertilizer on
688 biodegradation of crude oil by marine isolates of *Bacillus megaterium*,

689 *Corynebacterium kutscheri* and *Pseudomonas aeruginosa*. Bioresour. Technol. 102,
690 772-778.

691 Tsai, W.T., Chou, S.L., 2000. Environmentally assisted cracking behavior of duplex
692 stainless steel in concentrated sodium chloride solution. Corros. Sci. 42, 1741–1762.

693 Tsesmetzis, N., Alsop, E.B., Vigneron, A., Marcelis, F., Head, I.M., Lomans, B.P., 2016.
694 Microbial community analysis of three hydrocarbon reservoir cores provides valuable
695 insights for the assessment of reservoir souring potential. Int. Biodeterior. Biodegrad.
696 doi.org/10.1016/j.ibiod.2016.09.002.

697 Uzoigwe, C., Burgess, J.G., Ennis, C., Rahman, P.K.S.M., 2015. Bioemulsifiers are not
698 biosurfactants and require different screening approaches. Front. Microbiol. 6, 245.

699 Wade, S.A., Javed, M.A., Palombo, E.A., McArthur, S.L., Stoddart, P.R., 2017. On the need
700 for more realistic experimental conditions in laboratory-based microbiologically
701 influenced corrosion testing. Int. Biodeterior. Biodegrad. 121, 97-106.

702 Youssef, N., Elshahed, M.S., McInerney, M.J., 2009. Microbial processes in oil fields:
703 culprits, problems, and opportunities. Adv. Appl. Microbiol. 66, 141-251.

Figure Legends

Fig. 1. Neighbor-joining tree based on 16S rRNA gene sequences, showing phylogenetic relationships between sequences of the bacterial phylum *Firmicutes* (*Bacillus* related species) *Actinobacteria* (*Streptomyces* species). GenBank accession numbers are given in parentheses. The scale bar indicates sequence divergence.

Fig. 2. GC-MS analysis of biosurfactant from *S. parvus* B7 (a) GC spectrum of biosurfactant; (b) Mass spectra of n-hexadecanoic; (c) Mass spectra of octadecanoic acid and (d) Mass spectra of octadecanoic acid, methyl ester.

Fig. 3. FT-IR spectrum of partially purified biosurfactant isolated from *S. parvus* (B7).

Fig. 4. Bacterial growth curve of CDSs in BH medium with crude oil as a sole carbon source.

Fig. 5. Gas Chromatography mass spectrum (GC-MS) tracing of residual crude oil in the abiotic system control and experimental system (a) Abiotic system; (b) *B. pumilus* B1; (c) *B. subtilis* B5; (d) *B. megaterium* B6; (e) *S. parvus* B7 and (f) Mixed consortia.

Fig. 6. FT-IR spectrum of crude oil in abiotic control and experimental system inoculated with individual bacterial culture (a) Abiotic system; (b) *B. pumilus* B1; (c) *B. subtilis* B5; (d) *B. megaterium* B6; (e) *S. parvus* B7, and (f) Mixed consortia.

Fig. 7. Growth pattern of the mixed consortia in the bio-corrosion studies.

Fig. 8. Epi-fluorescence micrograph of bacterial biofilm (a) 2nd day (b) 4th day (c) 6th day (d) 8th day and (e) 10th day.

Fig. 9. Electrochemical analysis of the carbon steel API 5LX coupon exposed in different bio-corrosion studies; (a) Polarization curves and (b) Impedance curves (equivalent circuit was presented inside of the impedance curves).

Fig. 10. SEM micrograph of biofilm formation on carbon steel API 5LX surface coupon exposed in bio-corrosion studies; (a) Over view of the biofilm on metal surface and (b) Magnified view of the biofilm and bacterial attachments.

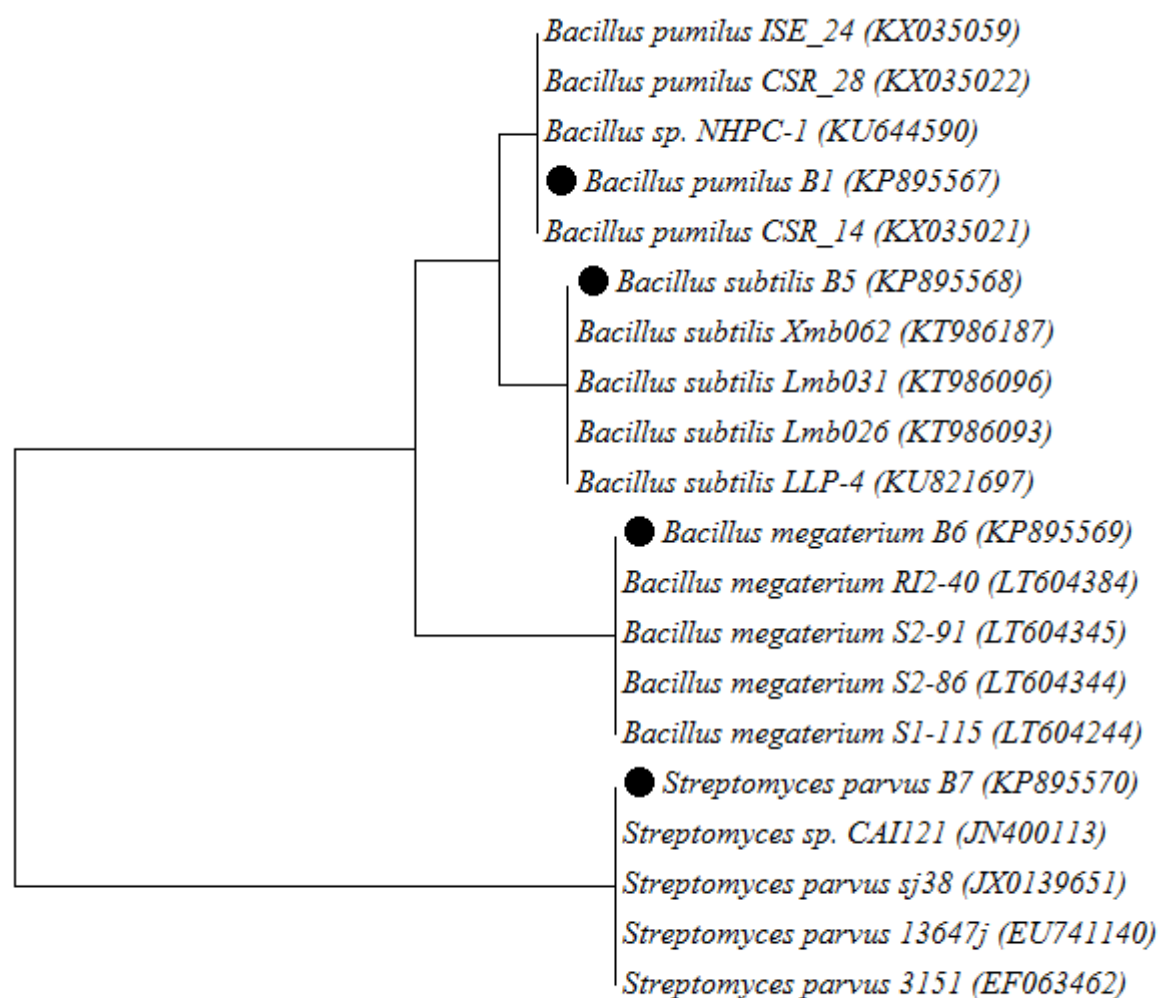
Fig. 11. SEM micrograph of typical pits formed on surface of the carbon steel API 5LX immersed in bio-corrosion studies; (a) abiotic control (bare metal) and (b) Mixed consortia.

Fig. 12. Two (a1 and b1), three (a2 and b2) dimensional images of the AFM observation of carbon steel API 5LX coupon surface show that pit formation on surface of the experimental systems in presence of mixed consortia, cross-sectional (a3 and b3) analysis determining the depth of pit on the metal surface.

Fig. 13. Analysis of corrosion product on carbon steel exposed to mixed bacterial consortia by XRD analysis (a) Abiotic system, and (b) Experimental system.

Fig. 14. FT-IR spectrum of surface film on the metal surface in presence/absence of mixed bacterial consortia (a) Abiotic system, and (b) Mixed consortia.

Fig. 1.



0.01

Fig. 2

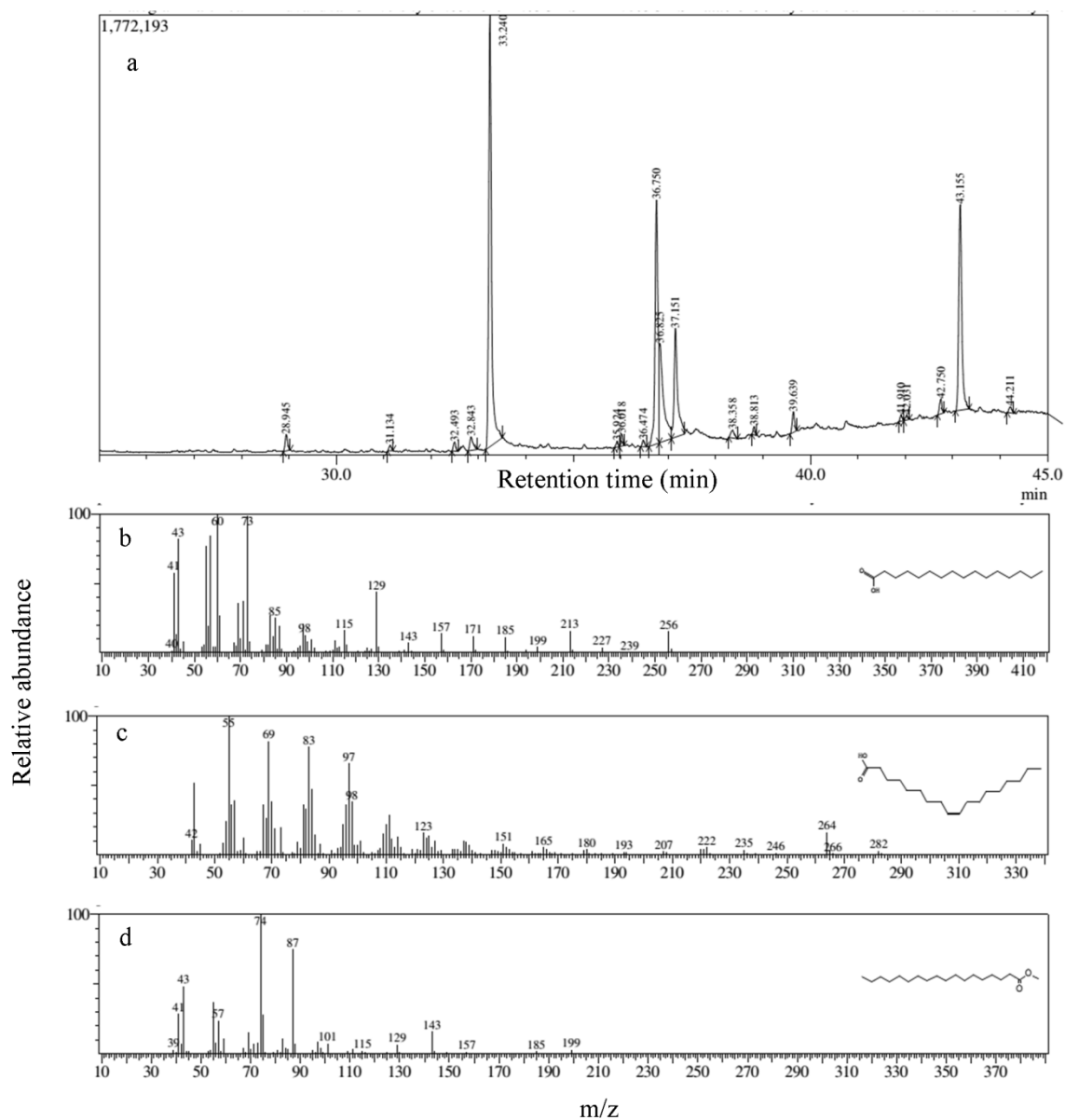


Fig. 3.

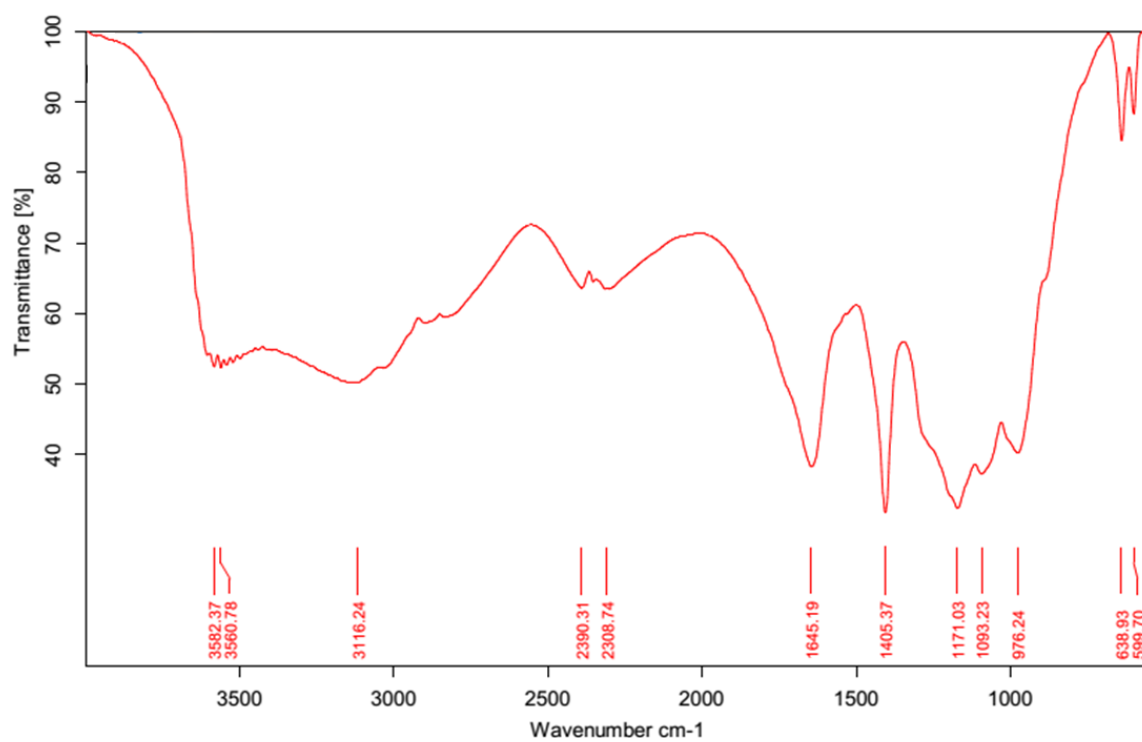


Fig. 4.

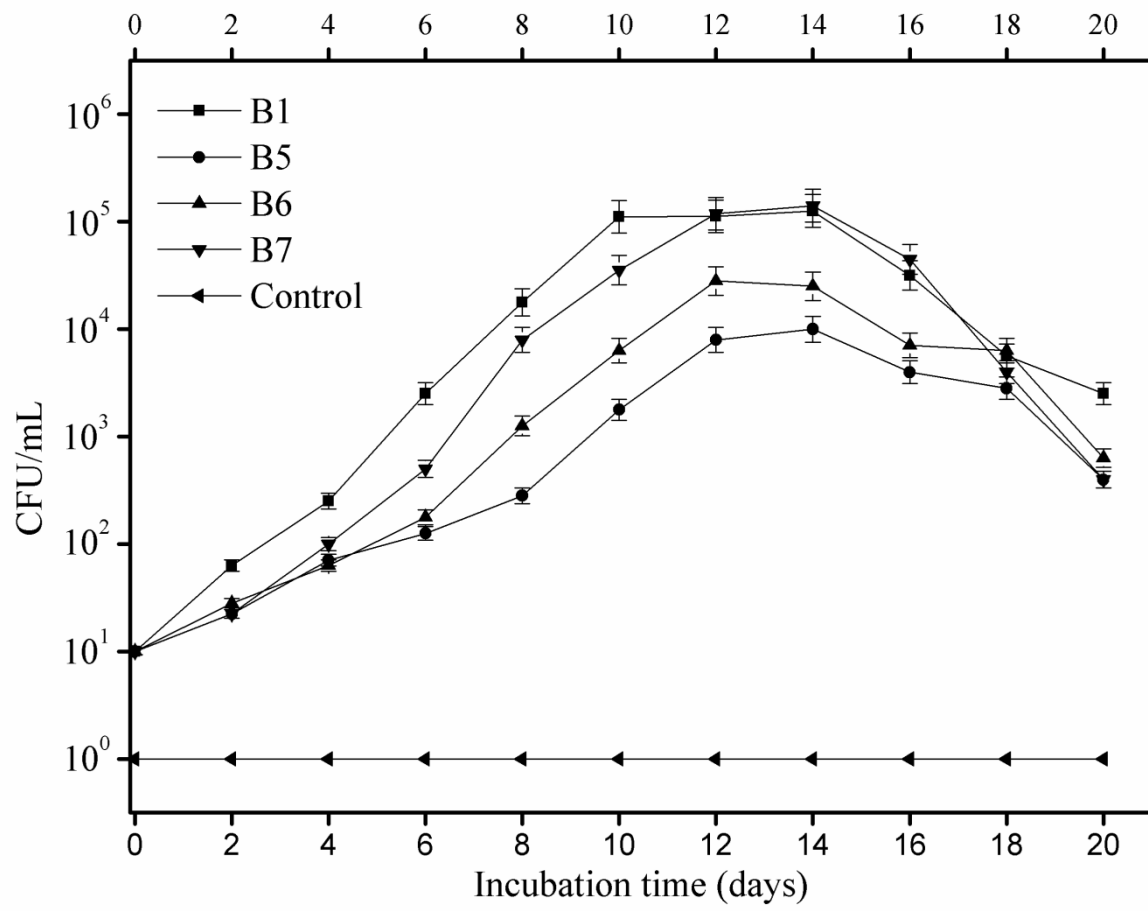


Fig. 5.

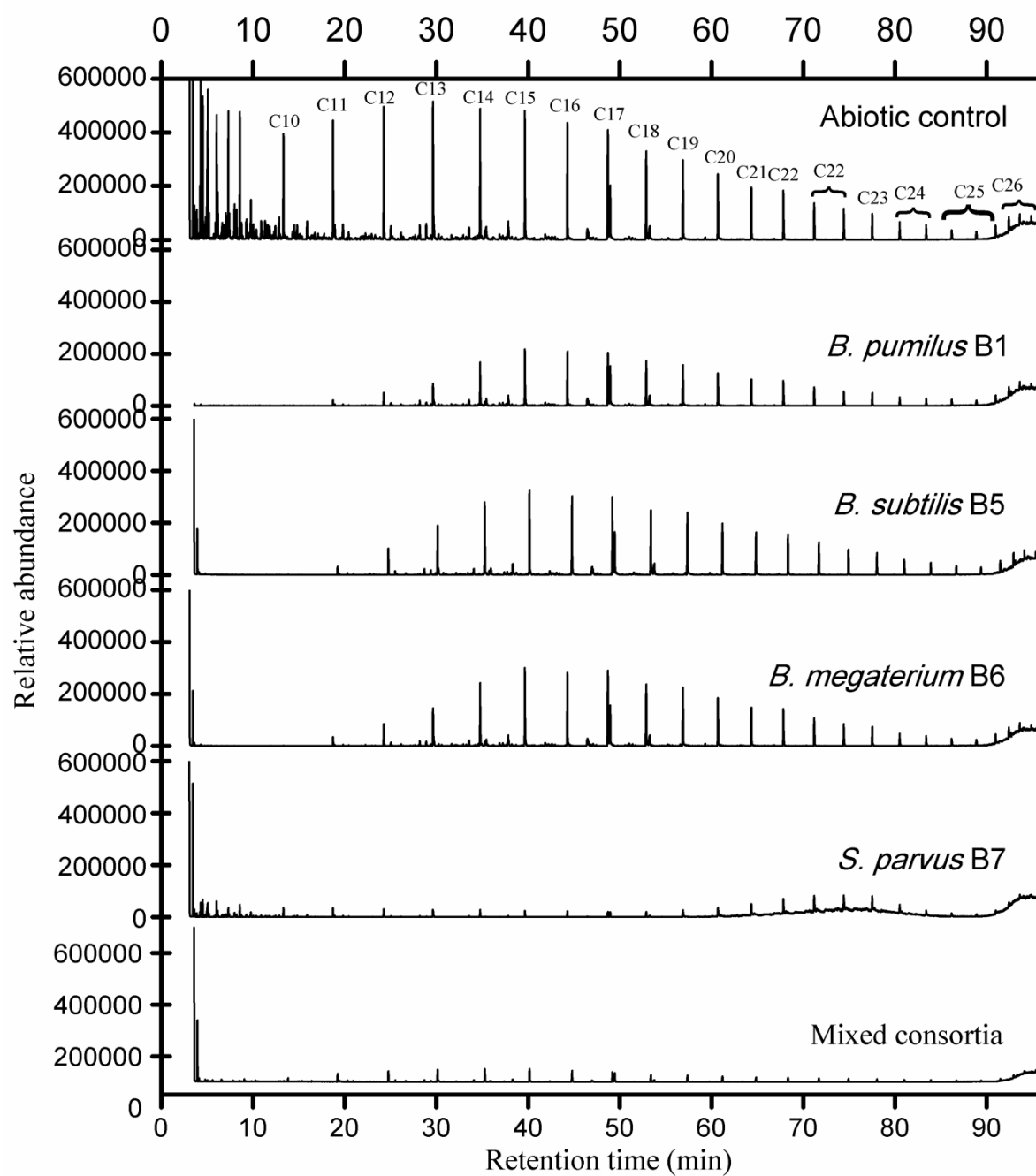


Fig. 6.

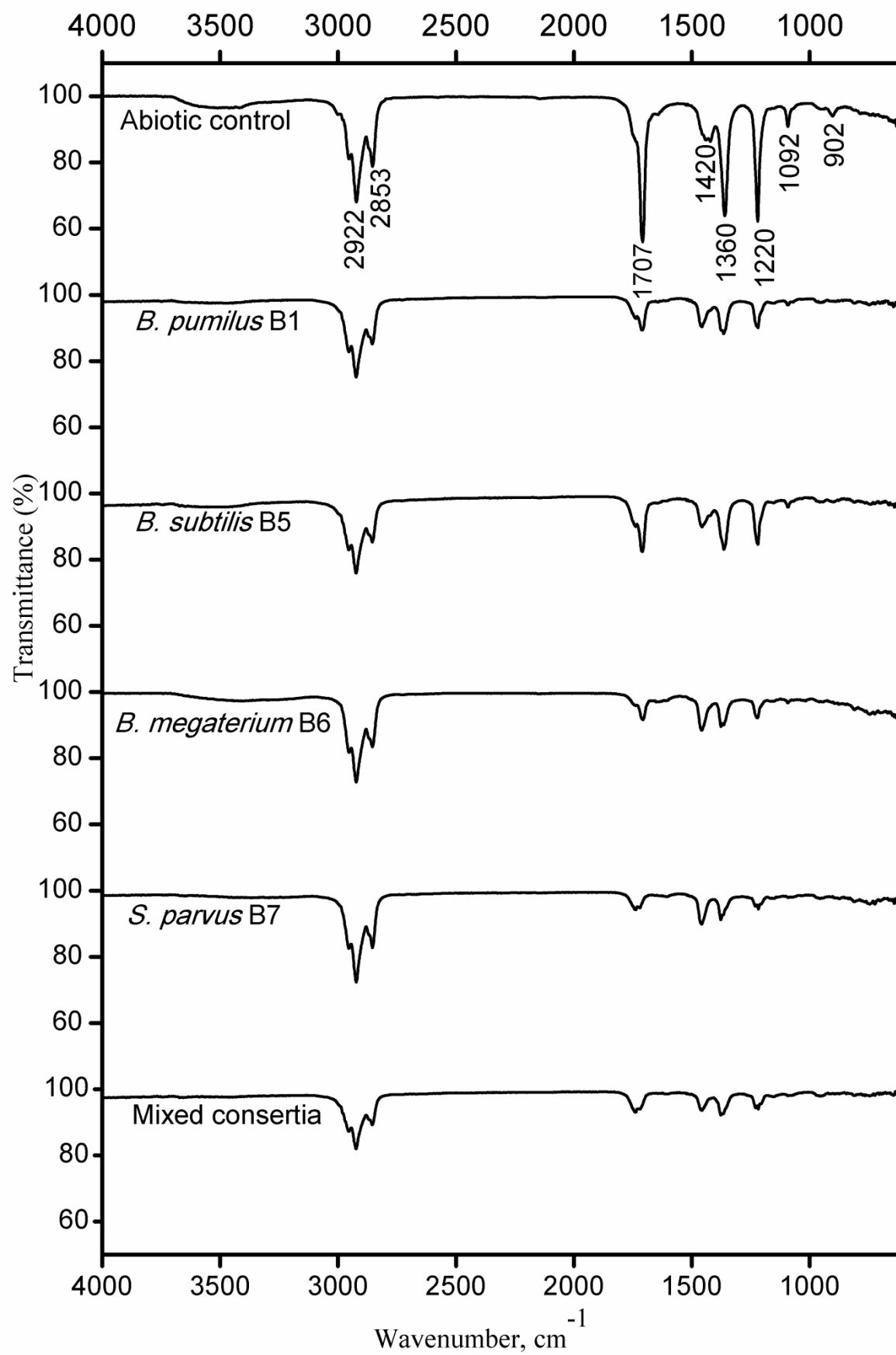


Fig. 7.

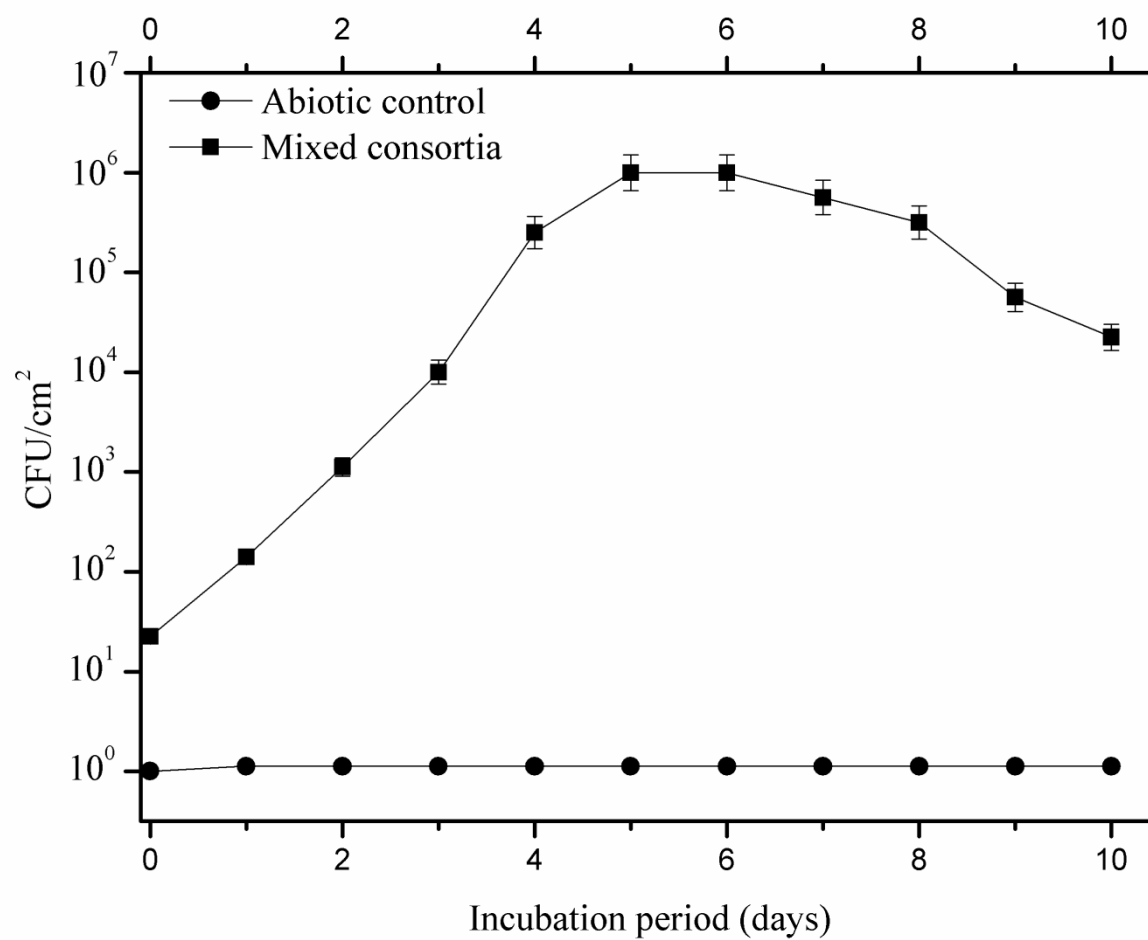


Fig. 8.

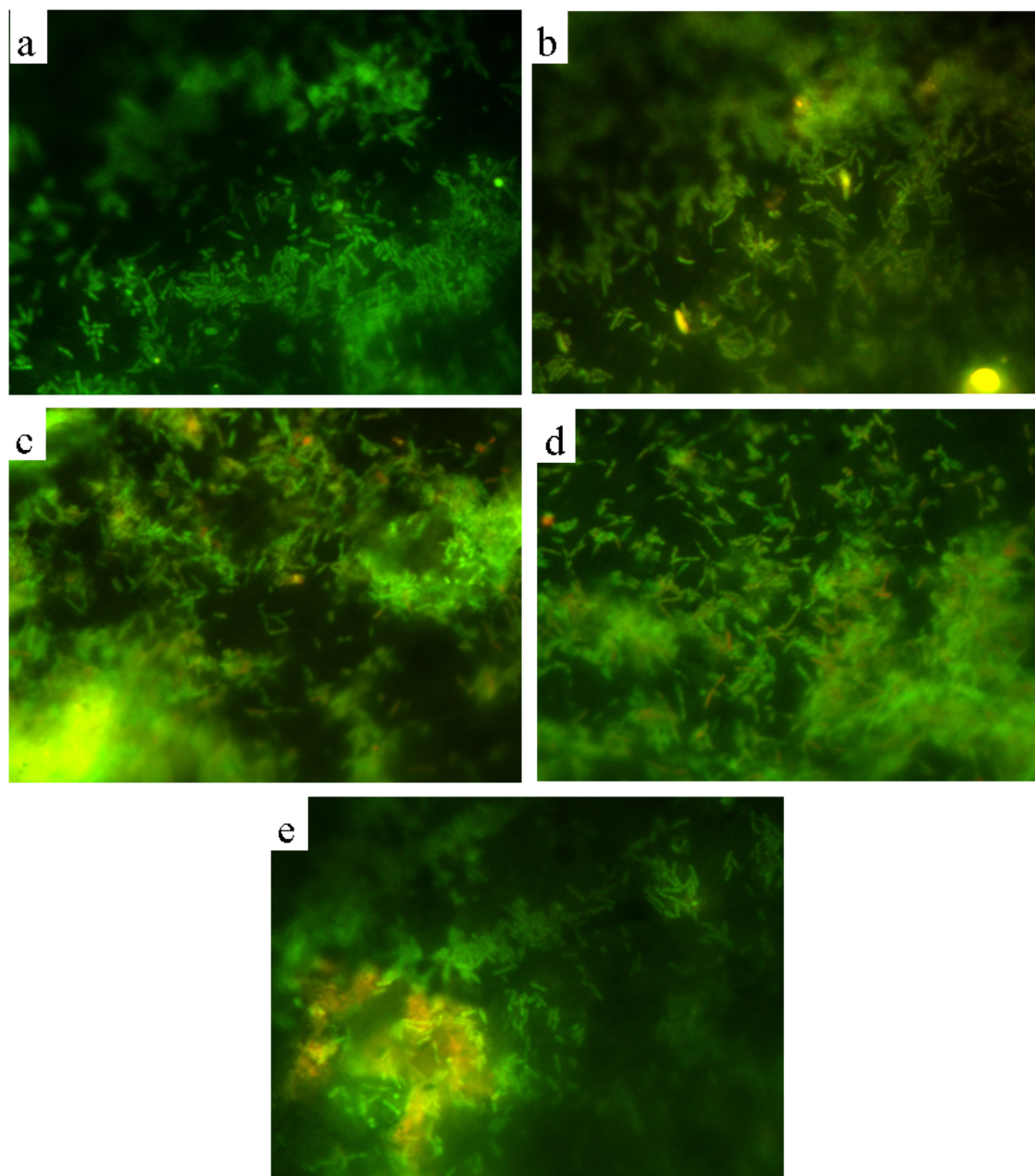


Fig. 9.

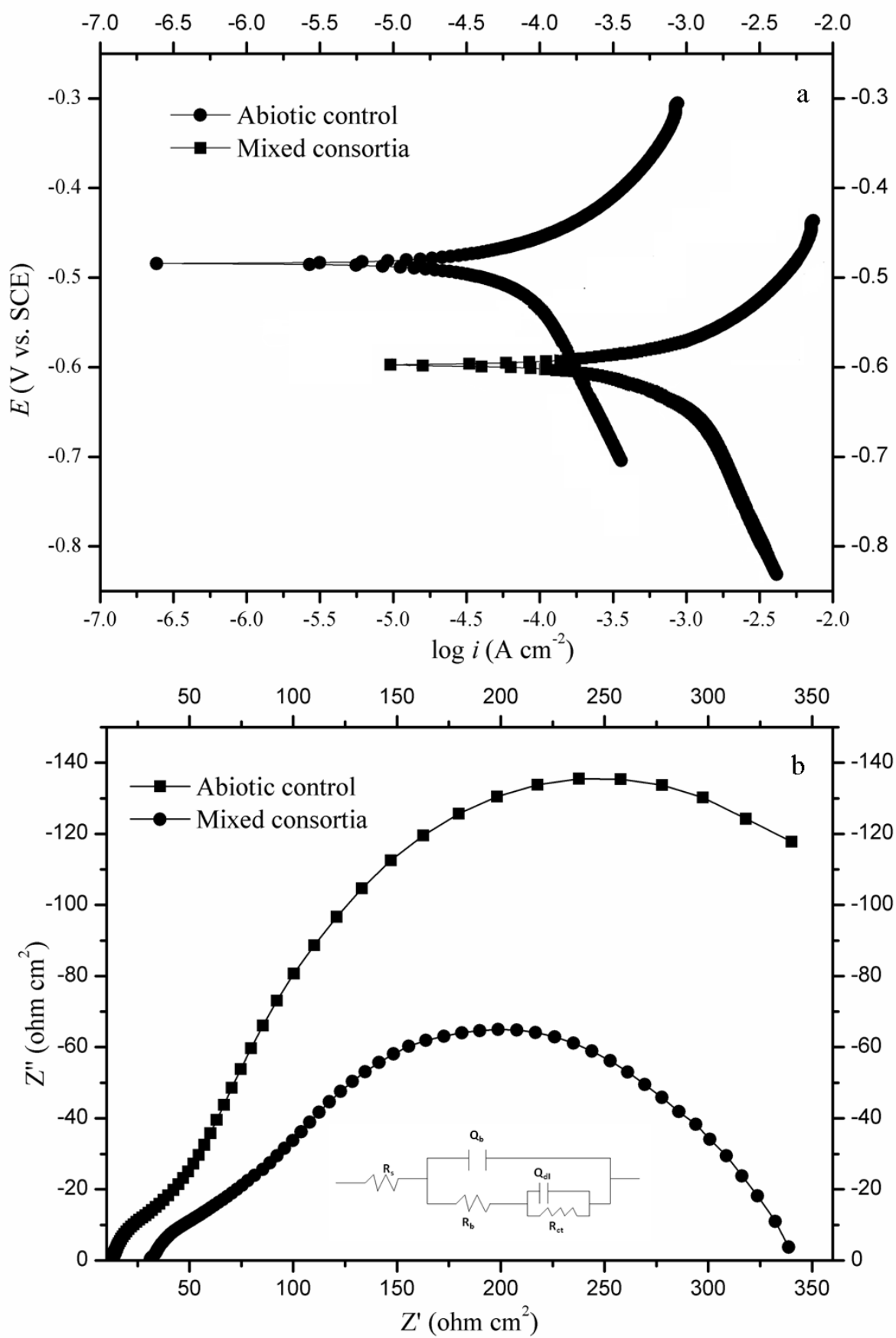


Fig. 10.

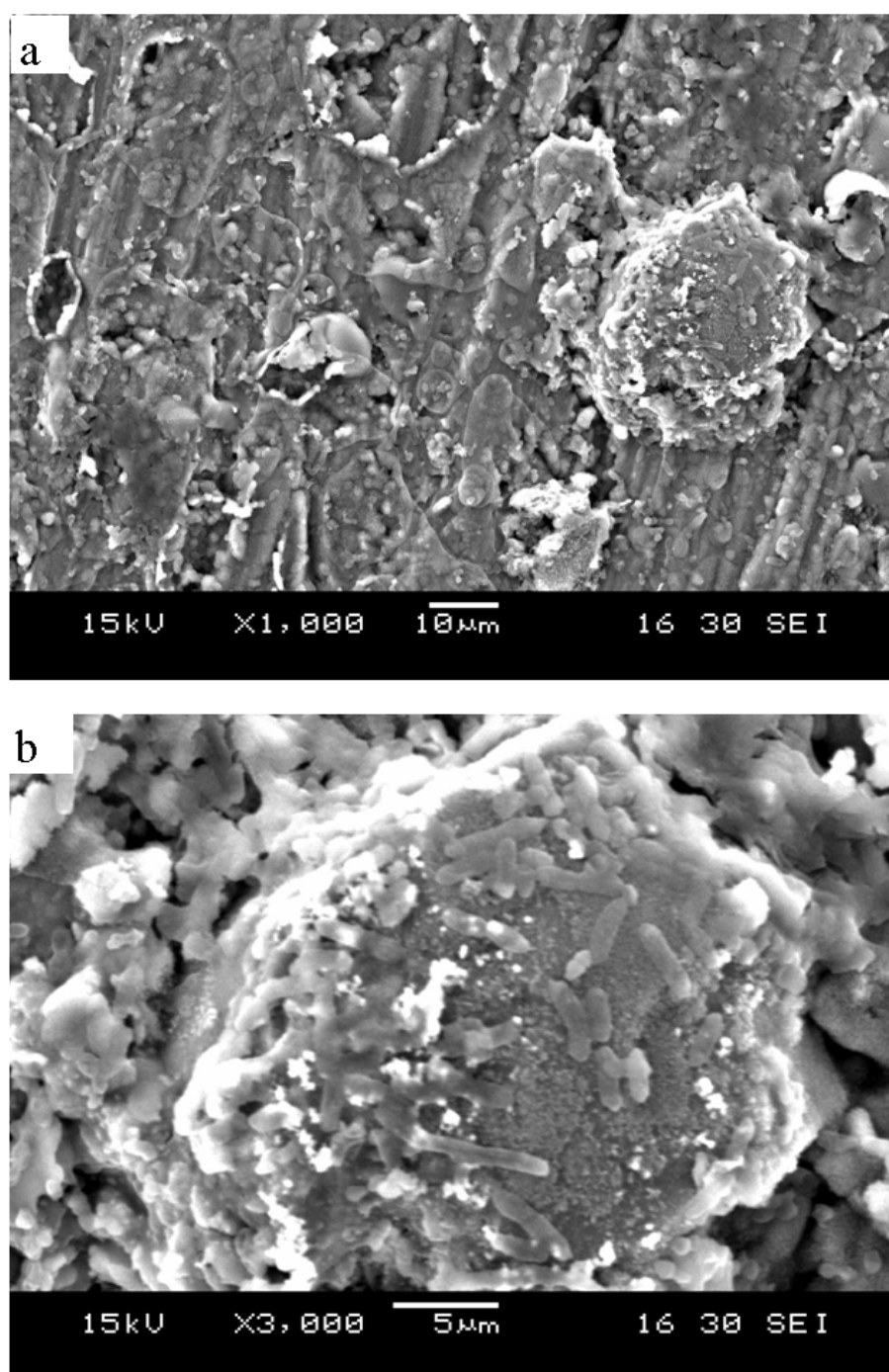


Fig. 11.

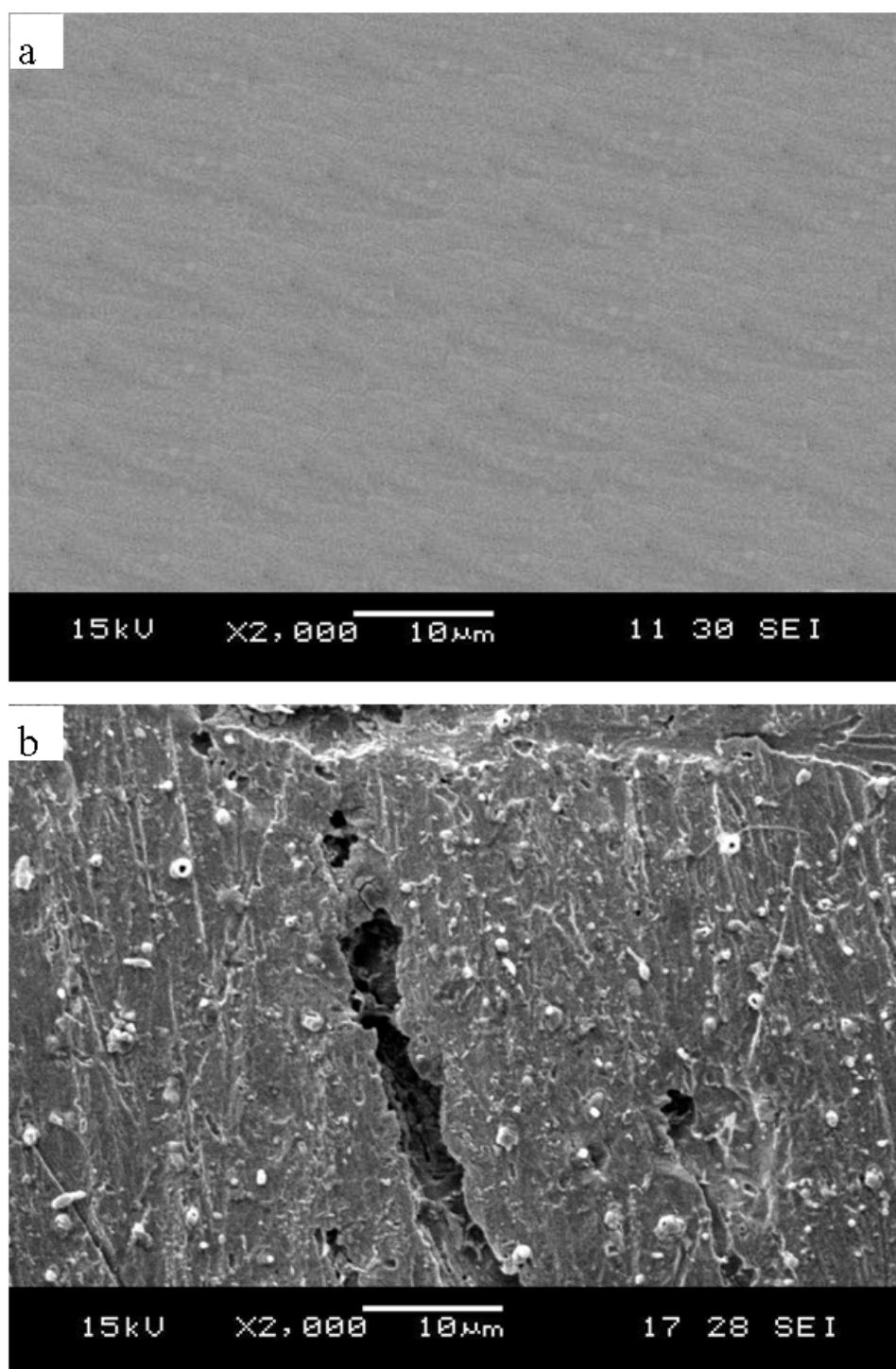


Fig. 12.

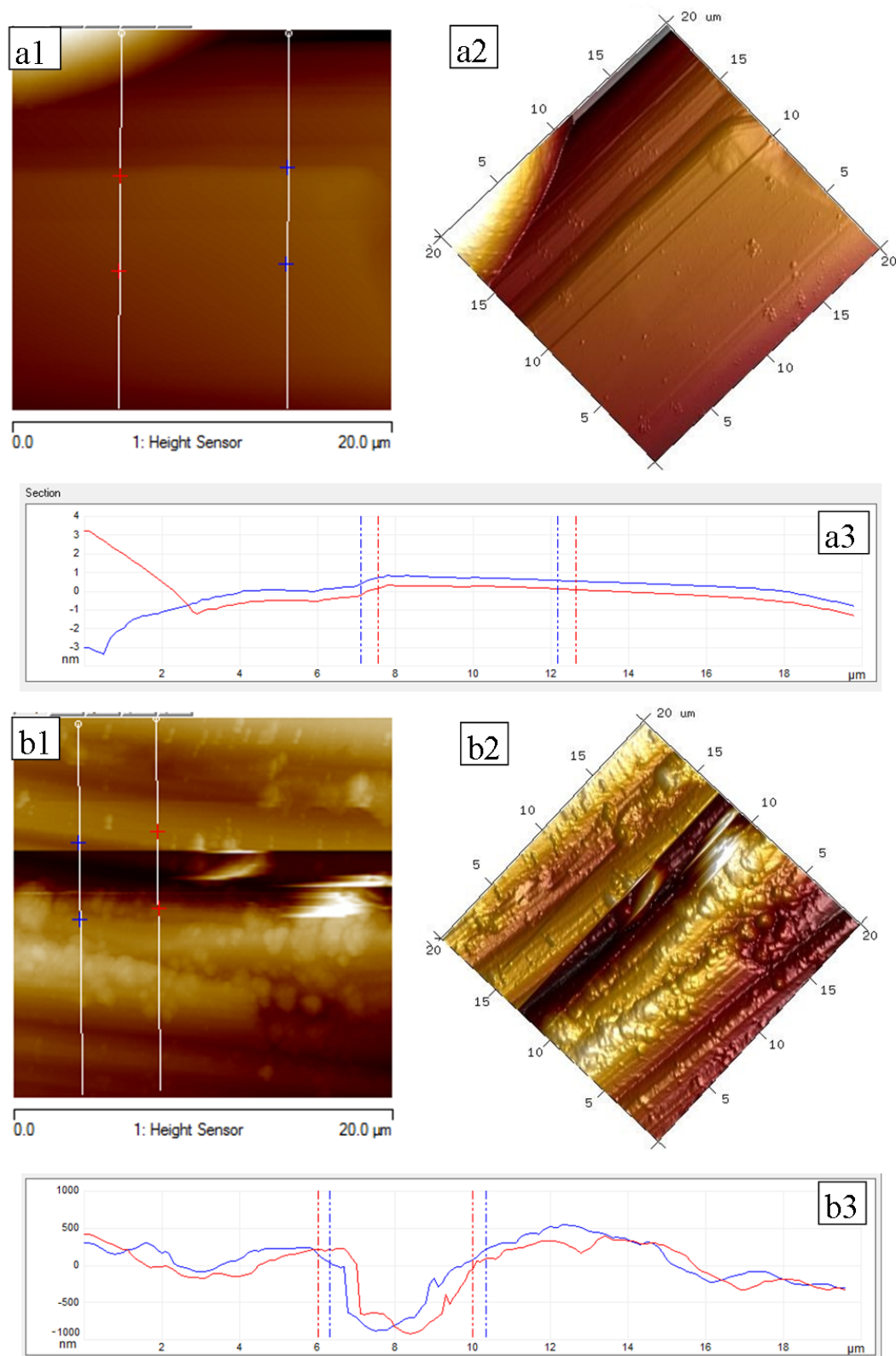


Fig. 13.

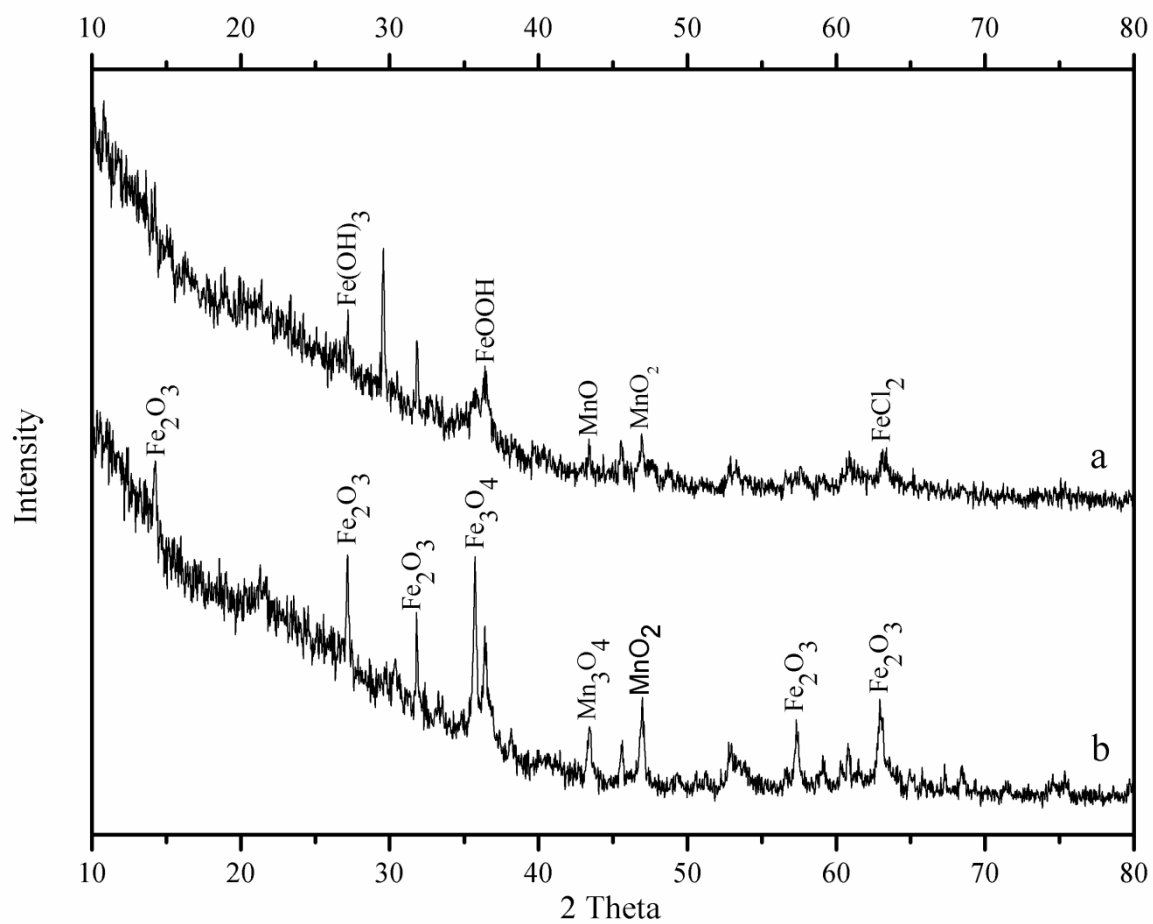


Fig. 14.

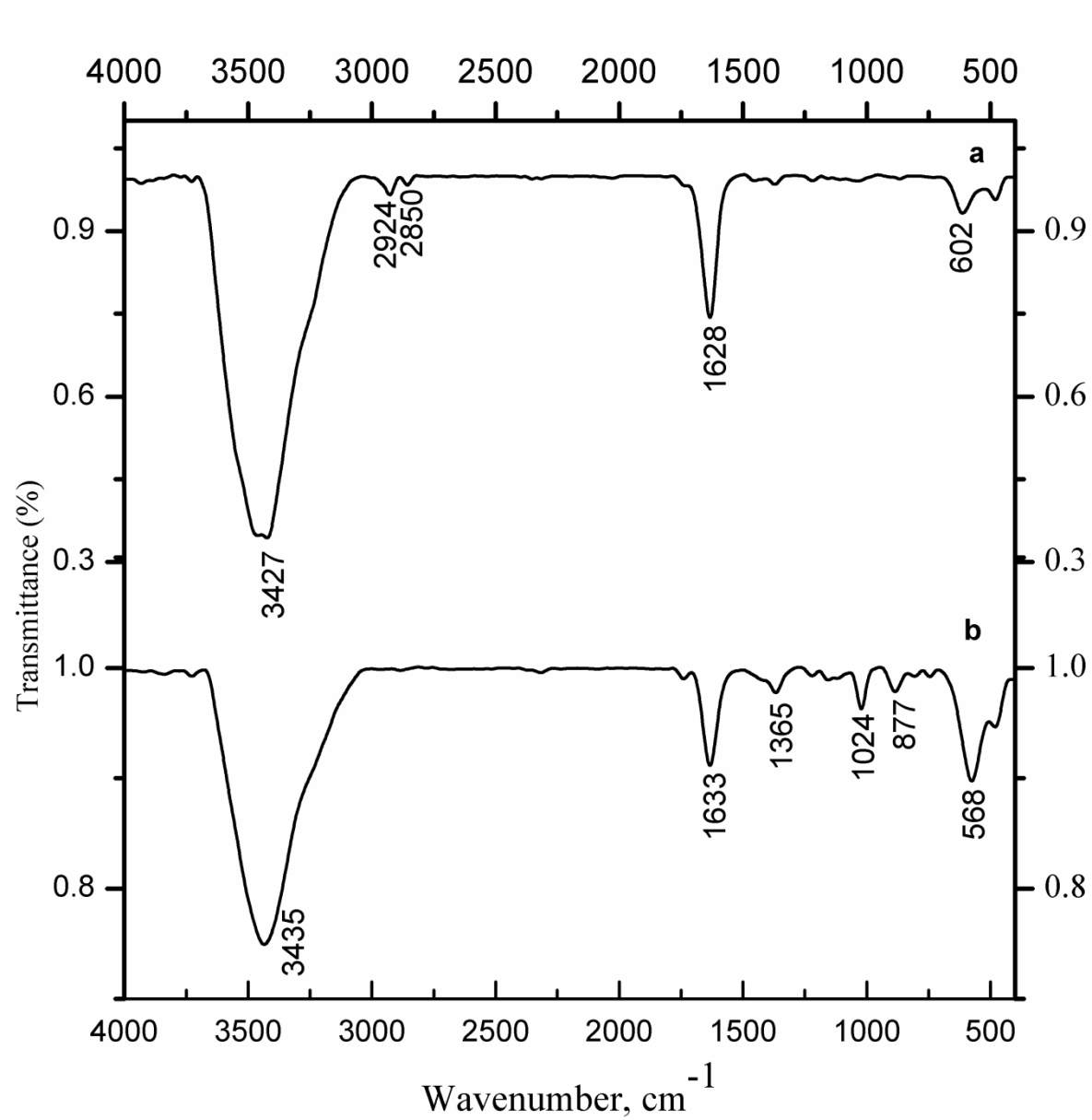


Table 1

Physiochemical characters of the produced water collected from Indian crude oil reservoir

S. No	Parameters	Present values (mg/L)
1	Total Suspended Solids	194
2	Oil & Grease	34.2
3	Total Dissolved Solids	59793
4	Salinity as NaCl	59303
5	Chloride as Cl ⁻	35988
6	Hardness as CaCO ₃	6700
7	Calcium as Ca ²⁺	1800
8	Magnesium as Mg ²⁺	529
9	Sodium as Na ⁺	20600
1	Iron as Fe ³⁺	32.9
11	Bicarbonate as HCO ₃ ⁻	525
12	Sulphate as SO ₄ ²⁻	354
13	pH	6.4

Table 2

Biochemical characterization of the CDSs isolated from Indian crude oil reservoir

Characteristics	B1	B5	B6	B7
Gram staining	+	+	+	+
Motility test	+	+	+	+
Indole Production test	-	-	-	-
Methyl red test	+	+	-	+
Voges-Proskauer test	+	+	+	+
Citrate test	-	+	-	-
Utilization of hydrocarbon				
Crude oil	+	+	+	+
Hexadecane	+	+	+	+
Production of acid from				
Glucose	-	+	+	+
Fructose	+	+	-	+
Dextrose	+	+	+	+
Sucrose	+	+	-	+
Catalase test	+	+	+	+
Oxidase test	+	+	+	+
Starch hydrolysis test	-	+	+	+
Gelatine	+	+	+	+

B1- *B. pumilus*, B5- *B. subtilis*, B6- *B. megaterium*, B7- *Streptomyces parvus*

Table 3

Screening for biosurfactant production: drop collapse assay, oil spreading assays and emulsification activity of the isolates

S. No	Name of bacteria	Hemolytic activity	Drop collapse assay	Oil spreading Assay	Emulsification index (E24%)
1	<i>B. pumilus</i> B1	+	++	++	33
2	<i>B. subtilis</i> B5	+	+	+	23
3	<i>B. megaterium</i> B6	+	+	+	26
4	<i>Streptomyces parvus</i> B7	+	+++	+++	46

Hemolytic activity: +, Positive response; -, Negative response

Drop collapse assay

‘+++’- Drop collapse within 1 minute, ‘++’- Drop collapse after 1minute and ‘+’ - Drop collapse after 2 minutes of biosurfactant addition.

Oil spreading assay

‘+’ - Oil spreading with a clear zone of 0.5-1.0 cm, ‘++’ - Oil spreading with a clear zone of 1.5 to 2.0 cm, ‘+++’ - Oil spreading with a clear zone of 2.0 to 3.0 cm.

Note: E24% checked using hexadecane.

Table 4

Percentage of biodegradation of crude oil the in presence of CDSs

RT	Compounds	RA	B1	BE(%)	B5	BE(%)	B6	BE(%)	B7	BE(%)	Mix	BE(%)	
3.0 & 3.5	2-methylpentane	100	0	100	0	100	0	100	0	100	0	100	
4.0	2,2-Dimethylpentane	100	0	100	0	100	0	100	11	89	1.4	99	
5.0	2,4- Dimethylpentane	92	0	100	0	100	0	100	9	90	1.4	98	
6.0	2-methylheptane	76	0	100	0	100	0	100	10	87	1.4	98	
7.3	Nonane	78	0	100	0	100	0	100	6	92	1	99	
8.5	Decane	78	0	100	0	100	0	100	7	91	2.8	96	
13.3	Undecane	66	0	100	0	100	0	100	6	91	2.8	96	
18.8	Dodecane	73	3	96	5	93	6	92	6	92	5	93	
24.2	Tridecane	82	9	89	15	82	14	83	5	94	7	91	
29.6	Decane	86	14	84	31	64	25	71	4	95	7.8	91	
34.6	2,3,5,8,tetramethyl Dodecane	2,6,10	81	28	65	53	35	40	51	4	95	8.5	90
39.5 & 44.2	trimethyl Hexadecane		76	35	54	49.5	35	48	37	3.7	95	7.7	89.5
48.7	Nonadecane		67	33	51	40	40	47	30	3.5	95	6	91
52.8	Octadecane		54	28	48	39	28	39	28	3.5	94	4	93
56.8	Nonadecane		49	25	49	29	41	37	24	4	92	4	92
60.6	Eicosane		41	21	49	27	34	30	27	6	85	2.8	93
64.3,67.8,71 .2,74.4,77.5 & 80.5	Eicosane-10-methyl		21.6	11	50.3	15.5	30.3	17	23.5	7.6	61.3	1.9	90
83.2, 86.1, 88.9 & 91.0	Heptadecane -9-octyl		6.5	3.6	43.7	4.8	21.7	4.8	25.2	2	69.2	1.2	81
92.4,93.5 & 94.8	Octadecane		6	3.2	42.6	3.3	44.3	4.1	30.6	1.6	71.6	1.4	75
Total biodegradation efficiency (%)				65.8		54.5		52.0		81.6		90.0	

Note: RT= Retention time, RA= Relative abundance (%), B1=*B. pumilus*, B5= *B. subtilis*, B6= *B. megaterium*, B7= *Streptomyces parvus*, Mix= Mixed consortia. Following compounds are given by mean values such as: 2-methylpentane, Hexadecane, Eicosane-10-methyl, Heptadecane -9-octyl and Octadecane.

Table 5

Corrosion rate of carbon steel in presence and absence of CDSs

Systems	Weight loss (mg)	Corrosion rate (mm/y)
Control system: 500 mL crude oil with 20% of produced water	40 ± 3	0.297 ± 0.020
Experimental system: 500 mL crude oil + 20% of produced water with mixed consortia	201 ± 2	1.493 ± 0.015

Table 6

Polarization and impedance parameters for carbon steel API 5LX in the presence/absence mixed bacterial consortia.

Systems	polarization data				impedance data		
	I_{corr} (A/cm ²)	E_{corr} (V vs. SCE)	β_a (mV/dec)	β_c (mV/dec)	R_{ct} ($\Omega \cdot \text{cm}^2$)	R_s (Ω)	R_b ($\Omega \text{ cm}^2$)
Control system:	$(1.2 \pm 0.15) \times 10^{-4}$	-495 ± 3	6.4 ± 0.3	-2.8 ± 0.2	21.3 ± 1	31 ± 1.2	-
500 mL crude oil with 20% produced water							
Experimental system: 500 mL crude oil with 20% produced water and mixed consortia	$(1.6 \pm 0.2) \times 10^{-3}$	-557 ± 2	9.3 ± 0.4	-3.8 ± 0.2	7.7 ± 0.8	11 ± 0.8	46 ± 2

E_{corr} - Corrosion potential, I_{corr} -Corrosion current, β_a - anodic tafel slope, β_c – cathodic tafel slope, R_s - Solution resistance, R_{ct} - Charge transfer resistance and R_b – Biofilm resistance.

Supplementary Information

Fig. S1. GC-MS analysis of biosurfactant from *B. pumilus* B1 (a) GC spectrum of biosurfactant; (b) Mass spectra of hexanedioic acid, bis (2-ethylhexyl) ester and (c) Mass spectra of palmitic acid.

Fig. S2. GC-MS analysis of biosurfactant from *B. subtilis* B5 (a) GC spectrum of biosurfactant and (b) Mass spectra of hexanedioic acid, bis (2-ethylhexyl) ester.

Fig. S3. GC-MS analysis of biosurfactant from *B. megaterium* B6 (a) GC spectrum of biosurfactant; (b) Mass spectra of hexanedioic acid, bis (2-ethylhexyl) ester and (c) Mass spectra of palmitic acid, methyl ester.

Fig. S1.

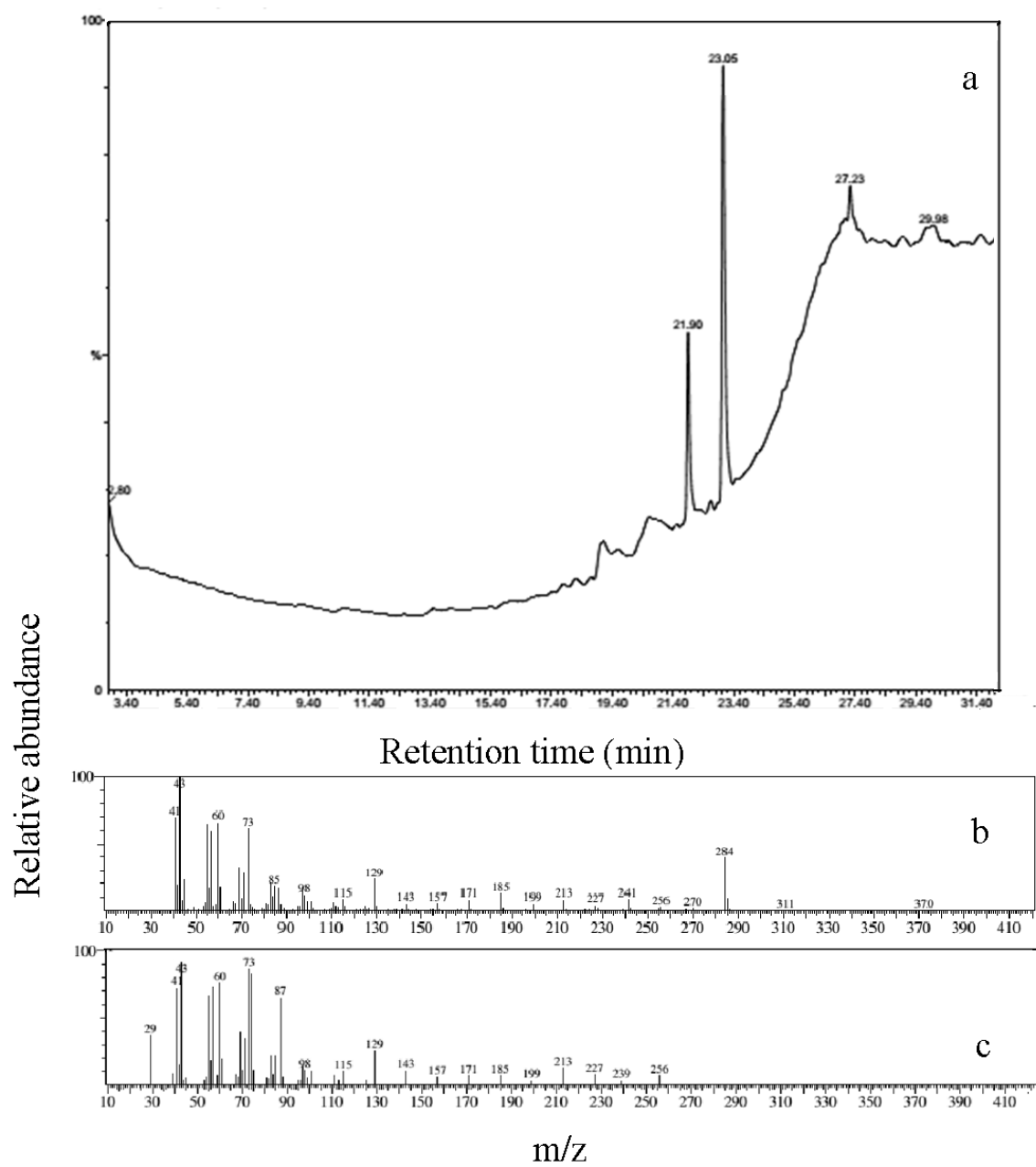


Fig. S2.

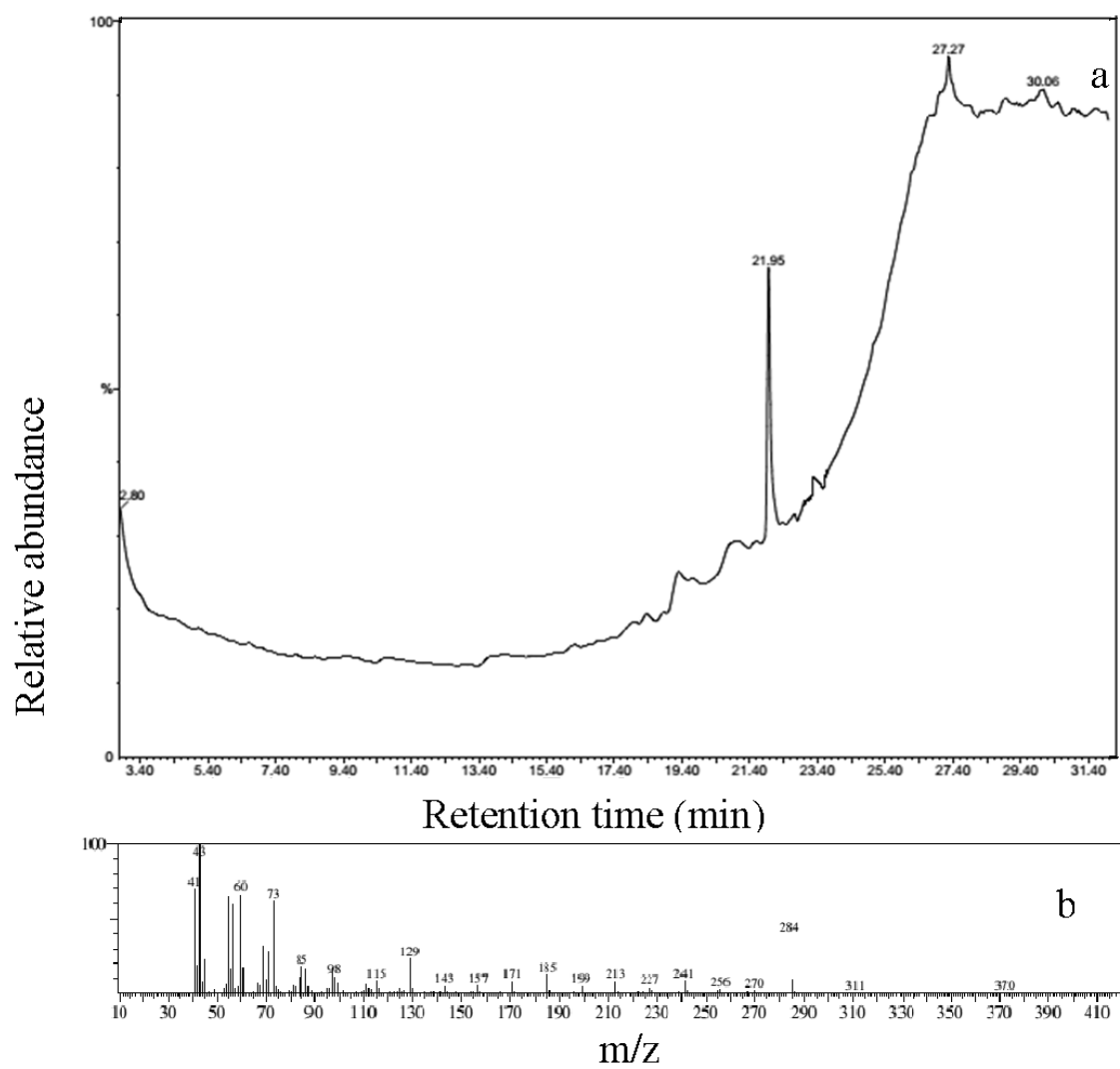


Fig. S3.

